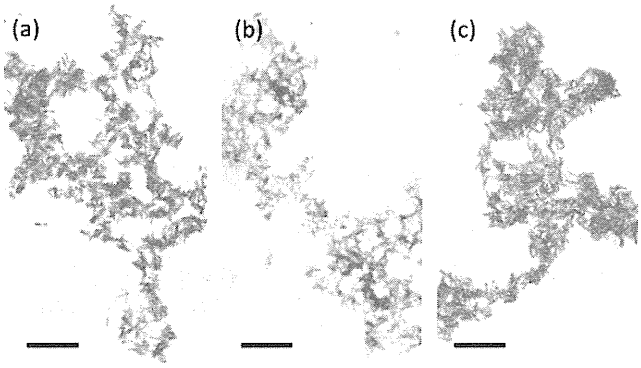

図4　結核菌の細胞壁ミコール酸合成に関わる *kasB* 遺伝子を欠損させた *kasB* knockout 株（b）と親株（a）および *kasB* 遺伝子を補完した株（c）の Ziehl-Neelsen 染色像．（b）の *kasB* knockout 株は細胞壁のミコール酸合成が正常に行われないため，抗酸性を消失して，フクシン色素が3%塩酸アルコールによる脱色で流出し，後染色のメチレンブルーにより青く染まっている．bar = 10 μm.

kasB 欠損変異株と親株，*kasB* 遺伝子を補完した株を入手し，Cryo-TEM で観察した．当初，ミコール酸伸長に関わる酵素活性を欠いた変異株は細胞壁構成成分であるミコール酸の長さが短くなるため，細胞壁の厚さが親株や補完株と比較して薄くなるだろうという仮説を立てた．しかし，実際に氷包埋サンプルで3株の細胞壁の厚さを測定したところ，株間に有意な差は見られなかった．菌体長，菌体幅，菌体全体の電子密度等のパラメーターを比較したがいずれも *kasB* 欠損株の抗酸性消失と相関するものはすぐには見つからなかった．様々なパラメーターの比較検討を試行錯誤した末，ミコール酸が存在すると思われる細胞壁の細胞膜と細胞壁外膜に挟まれた領域の電子密度が，*kasB* 欠損株で有意に低下していることが明らかになった．このことは，KasB の機能が欠損しているため，全体としてミコール酸合成が低下し，その密度が減少すると同時にβ鎖の伸長が不完全に終わるため，抗酸性が消失するが，相方の KasA が正常に機能しているために細胞壁の厚さに影響を及ぼさないと結論づけ，新たな細胞壁モデルを提唱した（図5）[23]．

今回の検討は，直接ミコール酸の局在部位を定量性を持って電子顕微鏡的に証明したものではないので，今後，ミコール酸を特異的に標識し電子顕微鏡で特定する手法の検討を試みたい．

5. コード形成

抗酸性と並んで結核菌のもう一つの形態学的特徴がコロニーのコード形成（cord formation）である．Tween 80 等の detergent を含まない液体培地や固形培地で培養された結核菌のコロニーを顕微鏡観察するとコード形成という極めて特徴的な形態を示す（図 1e，f）．図6は Löwenstein-Jensen 培地で4週間培養した結核菌コロニーを走査電子顕微鏡で観察したものである．倍率を上げて行くにつれて，個々の桿菌が長軸方向に並んで菌塊の束を形成し，それが重層して複雑なコロニー形態を形成しているのがわかる．コードは直線的に伸長することは稀で，束として湾曲することが多い．これは個々の菌が必ずしも完全な直線ではなく，やや湾曲した桿菌の形態を示すためと推察されるが，確固とした裏付けはない．また，隣接するコードがお互いに同調して湾曲しており，隣

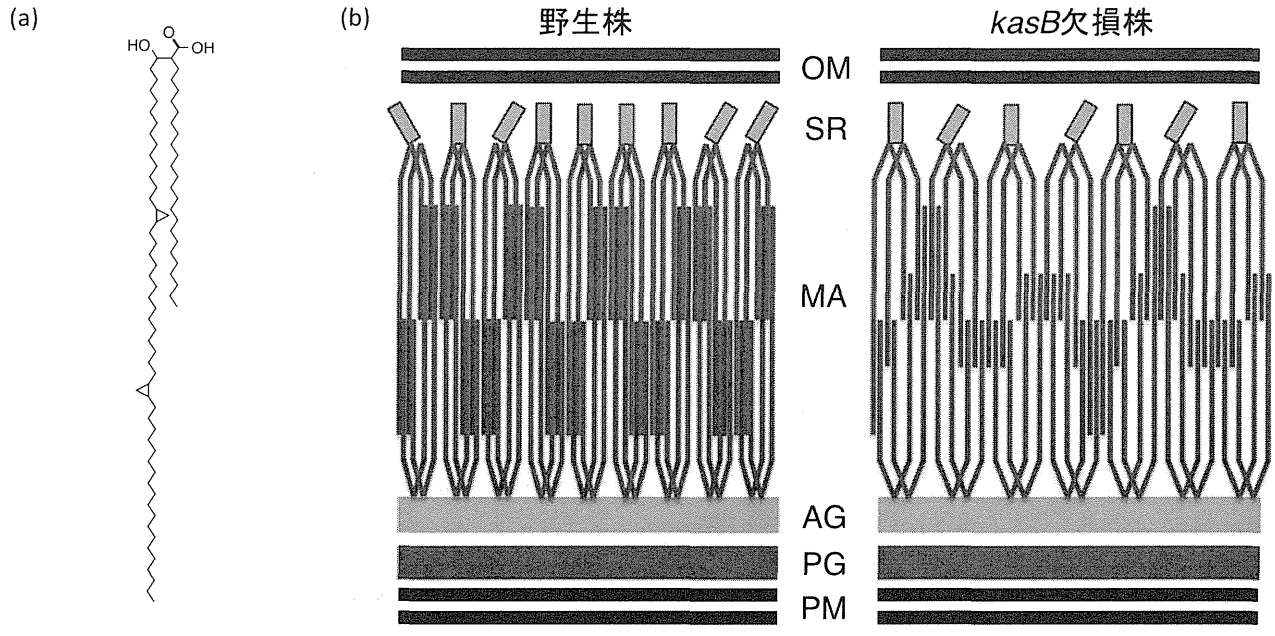

図5　結核菌の細胞壁ミコール酸の化学構造式（a）および結核菌野生株と *kasB* knockout 株の細胞壁のモデル（b）．変異株では KasB 酵素が欠損しているためミコール酸合成の総量が減少するとともに，β鎖（長い方の鎖）の伸長が正常に行われず，ミコール酸の密度が低下し，細胞壁の透過性が亢進して脱色されやすくなっている可能性が示唆された．OM：細胞壁外膜，SR：糖鎖，MA：ミコール酸，AG：アラビノガラクタン，PG：ペプチドグリカン，PM：細胞膜．

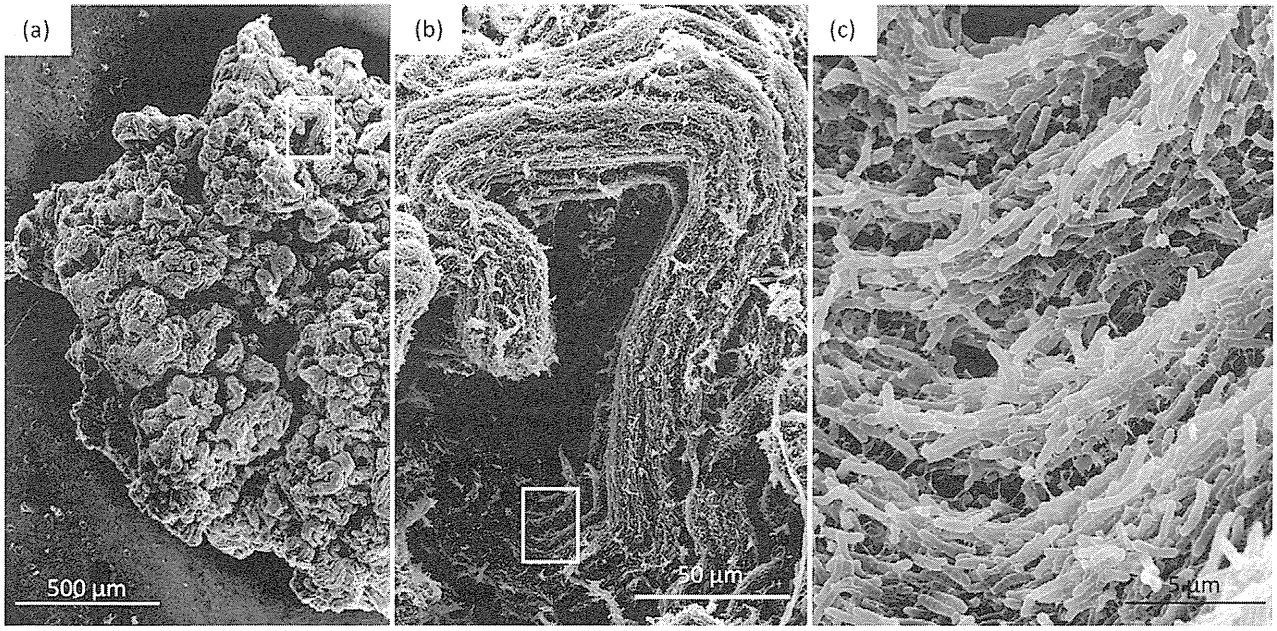

図6　Löwenstein-Jensen 培地で4週間培養した結核菌のコード形成を走査型電顕で観察した像．低倍率では明らかではないが（a，b），倍率を上げるに従って（b，c），個々の菌が隣接した菌と方向性を共有して並び，コードを形成しているのがわかる．また，隣接するコードが同調して方向性を示し，高次のコードを形成している．

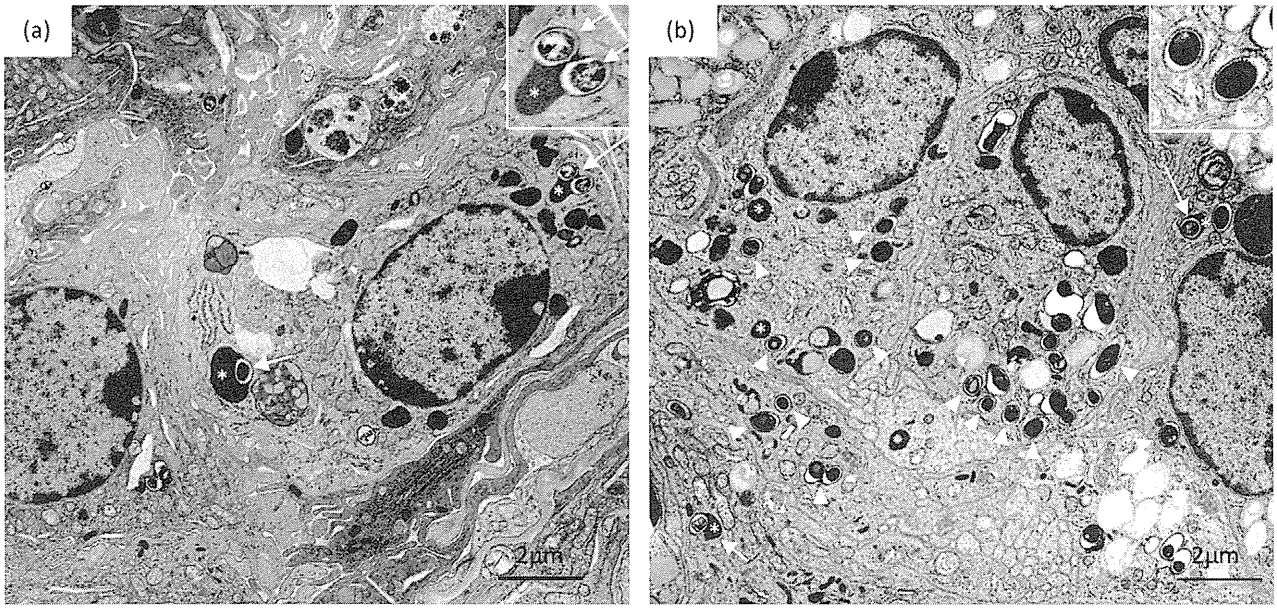

図7　結核菌を吸入感染したマウス肺病変の透過電子顕微鏡像．（a）野生型マウスの肺病変．菌（白矢印）の数が少なく，phagosome が lysosome（*）と融合（P-L fusion）している像が見られる．一方，（b）はサイトカンの転写発現に関わる転写因子 NF-κB p50 サブユニットを knockout したマウスの肺病変．細胞内に多数の菌を取り込んだ phagosome（白矢頭）が存在するが，lysosome（*）は遊離のものが多く，P-L fusion の像は数少ない（白矢印と *）．

接したコードの空間的な配置をどのように感知し，同調するための機序がどのように発現されるのかはコード形成自体の発現とともに，今後の研究の成果が期待される．

6. Phagosome-lysosome fusion

最後に紹介するのは感染宿主と結核菌の相互作用として最も重要な phagosome-lysosome fusion（P-L fusion）の透過電子顕微鏡観察像である．結核菌が感染しても実際に活動性の疾患として発病するのは感染者の10%以下であり，感染から発病までの潜伏期間が非常に長い．その潜伏期間における結核菌の局在と潜伏方法については不明な点が多いが，生存手段の1つとして，感染した貪食細胞内の phagosome 内部の酸性化を阻害して P-L fusion から巧みに逃れていることが想定されている．図7（a）は C57BL/6 野生型マウスに結核

菌を吸入感染させ，5週間後の肺病変を透過電子顕微鏡で観察したものである．白矢印で示したものは菌を取り込んだphagosomeとlysosome（白アスタリスク）が融合したP-L fusion像である．一方，図7（b）は転写因子NF-κBのp50サブユニットをknockoutしたマウスの感染5週目の肺病変の透過電顕像であるが，白矢頭で示したように結核菌を取り込んだ遊離のphagosomeが（a）と比較して多数存在するのに対し，遊離のlysosomeとP-L fusion像が少ないのがわかる．転写因子NF-κBはIFN-γやTNF-αなど多くのtype Iサイトカイン遺伝子の転写・発現に必須であり，NF-κB p50サブユニットの欠損によりこれらのサイトカイン発現が大きく減少して，殺菌作用が低下したためと考えられる[24]．

7. おわりに

今回，結核菌に関する形態学的特徴を光学顕微鏡，電子顕微鏡観察で得られたデータをもとに紹介させて頂いた．病原性が高い細菌ではあるがごく専門的な研究者により狭く深く調べられているため，一般には馴染みが薄い細菌ではないかと思う．昨今の可視化技術の進歩により，生命現象が視覚的に研究されることが多くなってきていることは喜ばしいが，それらの多くは真核細胞の観察を目的とされて開発されている．微生物分野，特に原核細胞を対象とした場合，光学顕微鏡観察により微生物の存在の有無（定量）や種類の鑑別（定性）の分析は可能である．しかし真核細胞のオルガネラに相当するサイズの微生物や細菌の細胞壁，細胞質の詳細な研究には電子顕微鏡を用いた観察が必須である．

細菌の細胞壁や細胞質の詳細な構造の解明，抗生物質やワクチンの実際の作用機序や作用部位の特定，未知の病原体の発見など，微生物学，細菌学の分野で電子顕微鏡が担う役割はますます大きくなると考えられる．今後，生化学的手法，分子生物学的手法と新旧の電子顕微鏡手法，装置との融合が期待される．この分野における本学会の役割も極めて重要であることは間違いない．

文　献

1) Iwai, K., Maeda, S. and Murase, Y.: *Kekkaku*, 85, 465–475 (2010)
2) Rothschild, B.M., Martin, L.D., Lev, G., Bercovier, H., Bar-Gal, G.K., Greenblatt, C., Donoghue, H., Spigelman, M. and Brittain, D.: *Clin. Infect. Dis.*, 33, 305–311 (2001)
3) Lee, O.Y., Wu, H.H., Donoghue, H.D., Spigelman, M., Greenblatt, C.L., Bull, I.D., Rothschild, B.M., Martin, L.D., Minnikin, D.E. and Besra, G.S.: *PLoS ONE*, 7, e41923 (2012)
4) Koch, R.: Nobel Prize Lecture, Dec. 12, 1905. (http://www.nobelprize.org/nobel_prizes/medicine/laureates/1905//koch-lecture.html)
5) 結核研究所疫学情報センター：「結核の統計」資料編（http://www.jata.or.jp/rit/ekigaku/toukei/adddata/）
6) World Health Organization: Global tuberculosis control 2012. (http://www.who.int/tb/publications/global_report/en/index.html)
7) 結核研究所疫学情報センター：結核の統計一年報（http://www.jata.or.jp/rit/ekigaku/toukei/nenpou/）
8) Mori, T., Mitarai, S. and Yoshiyama, T.: *Kekkaku*, 87, 565–575 (2012)
9) 抗酸菌検査法検討委員会（編）：結核菌検査指針2007，日本結核病学会，東京，52（2007）
10) Yamada, H., Mitarai, S., Wahyunitisari, M.R., Mertaniasih, N.M., Sugamoto, T., Chikamatsu, K., Aono, A., Matsumoto, H. and Fujiki, A.: *J. Clin. Microbiol.*, 49, 3604–3609 (2011)
11) Glickman, M.S.: in Daffé, M. and Reyrat, J-M. (Eds.) The mycobacterial cell envelope, ASM Press, Washington, DC, 63–73 (2008)
12) Paul, T.R. and Beveridge, T.J.: *J. Bacteriol.*, 174, 6508–6517 (1992)
13) Paul, T.R. and Beveridge, T.J.: *Infect. Immun.*, 62, 1542–1550 (1994)
14) Amako, K., Takade, A., Umeda, A., Matsuoka, M., Yoshida, S. and Nakamura, M.: *Microbiol. Immunol.*, 47, 387–394 (2003)
15) Hoffmann, C., Leis, A., Niederweis, M., Plitzko, J.M. and Engelhardt, H.: *Proc. Natl. Acad. Sci. USA*, 105, 3963–3967 (2008)
16) Zuber, B., Chami, M., Houssin, C., Dubochet, J., Griffiths, G. and Daffé, M.: *J. Bacteriol.*, 190, 5672–5680 (2008)
17) Sani, M., Houben, E.N., Geurtsen, J., Pierson, J., de Punder, K., van Zon, M., Wever, B., Piersma, S.R., Jimenez, C.R., Daffé, M., Appelmelk, B.J., Bitter, W., van der Wel, N. and Peters, P.J.: *PLoS Pathog*, 6, e1000794 (2010)
18) Yamada, H., Mitarai, S., Chikamatsu, K., Mizuno, K. and Yamaguchi, M.: *J. Microbiol. Methods*, 80, 14–18 (2010)
19) Yamaguchi, K., Suzuki, K. and Tanaka, K.: *J. Electron. Microsc.*, 59, 113–118 (2010)
20) Bhatt, A., Kremer, L., Dai, A.Z., Sacchettini, J.C. and Jacobs, W.R., Jr.: *J. Bacteriol.*, 187, 7596–7606 (2005)
21) Bhatt, A., Fujiwara, N., Bhatt, K., Gurcha S.S., Kremer, L., Chen, B., Chan, J., Porcelli, S.A., Kobayashi, K., Besra, G.S. and Jacobs, W.R., Jr.: *Proc. Natl. Acad. Sci. USA*, 104, 5157–5162 (2007)
22) Bhatt, A., Molle, V., Besra, G.S., Jacobs, W.R., Jr. and Kremer, L.: *Mol. Microbiol.*, 64, 1442–1454 (2007)
23) Yamada, H., Bhatt, A., Danev, R., Fujiwara, N., Maeda, S., Mitarai, S., Chikamatsu, K.. Aono, A., Nitta, K., Jacobs, W.R., Jr. and Nagayama, K.: *Tuberculosis*, 92, 351–357 (2012)
24) Yamada, H., Mizuno, S., Reza-Gholizadeh, M. and Sugawara, I.: *Infect. Immun.*, 69, 7100–7105 (2001)

Journal of Microbiological Methods 96 (2014) 50–55

Contents lists available at ScienceDirect

Journal of Microbiological Methods

journal homepage: www.elsevier.com/locate/jmicmeth

Pre-fixation of virulent *Mycobacterium tuberculosis* with glutaraldehyde preserves exquisite ultrastructure on transmission electron microscopy through cryofixation and freeze-substitution with osmium-acetone at ultralow temperature

Hiroyuki Yamada *, Kinuyo Chikamatsu, Akio Aono, Satoshi Mitarai

Department of Mycobacterium Reference and Research, Research Institute of Tuberculosis, Japan Anti-Tuberculosis Association, 3-1-24 Matsuyama, Kiyose, Tokyo 204-8533, Japan

ARTICLE INFO

Article history:
Received 1 July 2013
Received in revised form 22 October 2013
Accepted 24 October 2013
Available online 4 November 2013

Keywords:
Mycobacterium tuberculosis
Virulent strain
Freeze-substitution
Transmission electron microscopy
Glutaraldehyde fixation

ABSTRACT

Sample preparations for transmission electron microscopy of virulent *Mycobacterium tuberculosis* are usually performed with chemical fixation using glutaraldehyde (GA) in a biosafety area followed by post-fixation with aqueous osmium tetroxide (OT) in a conventional laboratory outside the biosafety area. Freeze-substitution with osmium-acetone (OA) at ultralow temperature (−85 °C) has been shown to provide high quality final images and preserves cellular structures intact. However, some preparation procedures for freeze-substitution often require large fixed devices for freezing in a special laboratory. We have reported a novel freeze-substitution preparation method that can be performed using a portable device in a biosafety cabinet at biosafety level (BSL) 3 areas. Here, as a next step, we examined whether images obtained from rapid freeze-substitution (RFS) after fixation with glutaraldehyde (GA > RFS) are of comparable quality to those obtained using standard RFS. GA > RFS provided excellent preservation of mycobacterial cell ultrastructure, including visualization of cytoplasmic ribosomes, DNA fibers, and the outer membrane. The average number of ribosomes per cubic micrometer counted on RFS and GA > RFS was not significantly different (6987.8 ± 2181.0 and 6888.9 ± 1799.3, respectively). These values were higher, but not significantly so, than those obtained using conventional chemical fixation (5018.7 ± 2511.3). This procedure may be useful for RFS preparation of unculturable mycobacteria strains or virulent strains isolated in laboratories that cannot perform RFS.

1. Introduction

In the field of mycobacterial microscopy, novel procedures are being developed at an increasing pace. For example, microfluidic cultures and time-lapse microscopy have been developed to track the life cycle of a single live cell (Aldridge et al., 2012; Golchin et al., 2012; Wakamoto et al., 2013), and cryo-electron microscopy techniques such as specimen vitrification in ice followed by cryo-electron microscopy of vitreous sections (CEMOVIS), without specimen fixation or staining have been developed to observe fully hydrated bacterial cells (Matias and Beveridge, 2006; Hoffmann et al., 2008; Zuber et al., 2008; Coutre-Tosi et al., 2010; Hurbain and Sachse, 2011; Perez-Cruz et al., 2013). Although both procedures provide live images of the intact ultrastructure of biological materials, they are performed without chemical fixation, which limits their use to nonpathogenic bacteria outside of strict biosafety facilities.

In several previous electron microscopy studies of mycobacteria, bacilli grown on solid media were embedded in melted agar and subjected to the impact freezing method (Amako et al., 2003; Paul and Beveridge, 1992, 1994; Takade et al., 2003). In our previous study, we reported a novel rapid freeze-substitution (RFS) procedure that was applicable to highly virulent *Mycobacterium tuberculosis* strains inside a class IIB biosafety cabinet at a biosafety level 3 facility and that met all biosafety requirements (Yamada et al., 2010). In this procedure, agar-embedding steps were excluded in order to preserve the ultrastructure intact, as far as possible. Instead, a small volume of highly concentrated bacillary solution was sandwiched between two single-holed copper grids and immediately immersed in melting propane. The bacilli were quickly fixed and substituted at ultralow temperature (−85 °C) with 2% osmium tetroxide (OsO_4, OT) dissolved in acetone (Yamada et al., 2010, 2012).

In this study, we report that the abovementioned pre-fixation procedure with glutaraldehyde (GA) followed by RFS at ultralow temperature with an osmium-acetone (OA) solution can preserve the exquisite ultrastructure of tubercle bacilli. It had been thought that GA fixation or chemical fixation (CF) performed with a combination of GA and OT

Abbreviations: BSL, biosafety level; CEMOVIS, cryo-electron microscopy of vitreous section; CF, chemical fixation; CF > RFS, rapid freeze-substitution after chemical fixation; GA, glutaraldehyde; GA > RFS, rapid freeze-substitution after glutaraldehyde fixation; MDR, multidrug-resistance; OA, osmium-acetone; OT, osmium tetroxide; PB, phosphate buffer; RFS, rapid freeze-substitution; TEM, transmission electron microscopy; XDR, extensively drug-resistant.

* Corresponding author. Tel.: +81 42 493 5072; fax: +81 42 492 4600.
E-mail address: hyamada@jata.or.jp (H. Yamada).

0167-7012/$ – see front matter © 2013 Elsevier B.V. All rights reserved.
http://dx.doi.org/10.1016/j.mimet.2013.10.019

could cause the ultrastructure to deteriorate. However, we demonstrate here that both pre-fixation of tubercle bacilli with GA before rapid freezing and cryofixation/substitution with OA substitution at ultralow temperature are crucial to preserving the ultrastructure. These results indicate that poor preservation of ultrastructure should be attributed to gradual freezing or OT fixation at a relatively higher temperature (even at 4 °C) than ultralow temperature. In the improved technique reported here, pathogenic bacilli were fixed with GA in a biosafety area, and could then be immediately transferred to a conventional laboratory desktop and subjected to rapid freezing and cryofixation/substitution with OA. This procedure is extremely useful for RFS sample preparation of highly biohazardous multidrug-resistant (MDR) or extensively drug-resistant (XDR) isolates, viable but nonculturable isolates, and samples isolated in locations where RFS cannot be performed in situ before transportation to an RFS-compatible laboratory.

2. Materials and methods

2.1. Bacteria

M. tuberculosis H37Rv (ATCC 25618) was cultured with Middlebrook 7H9 (Becton Dickinson, MD, USA) supplemented with oxalic acid, albumin (fraction V), dextrose and catalase (OADC) enrichment (Becton Dickinson, MD, USA), and 0.05% Tween 80 for 2 weeks. One-milliliter aliquots were transferred to sterile microcentrifuge tubes and centrifuged at 10,000 ×*g* for 1 min. Supernatants were discarded, and the remaining pellets were collected in two microcentrifuge tubes. One aliquot of the pellet was used for original RFS and another was either subjected to GA fixation alone or processed using conventional CF with GA and 1% OT and RFS after GA or CF as described below. All steps involving live virulent bacteria were performed in a biosafety cabinet at a biosafety level 3 facility.

2.2. Fixation

2.2.1. Pre-GA fixation and conventional CF

A highly concentrated bacillary pellet obtained as above was fixed with 2.5% GA in 0.1 M phosphate buffer (PB, pH 7.4) at 4 °C for at least 2 h. After centrifugation, the supernatant was discarded and rinsed with PB three times, after which the sample was divided into two microcentrifuge tubes. One part of the sample was subjected to RFS as described below (Fig. 1b) and the other was subjected to 1% aqueous OT fixation as conventional CF at 4 °C for 1 h. After OT fixation, the latter sample was rinsed with PB and one aliquot was subjected to rapid freezing in the same manner as the RFS described below (Fig. 1c) while the other was transferred to absolute acetone and stored in a freezer at −85 °C without rapid freezing. The remaining sample was prepared using conventional CF (Fig. 1d).

2.2.2. RFS

The sandwich method was performed as described (Yamada et al., 2010; Yamaguchi et al., 2003, 2009) and is summarized in Fig. 1a–d. Briefly, volumes of less than 1 μl of the highly concentrated bacillary pellets that were either not chemically fixed or were GA/CF fixed were applied to glow-discharge-treated single-hole copper grids (hole size 0.1 mm diameter; Veco, Eerbeek, Netherlands), then pellets were covered with another grid. Using tweezers, the grids were then immersed in melting propane for 20 s before being placed in the cooling device (Model VFZ-101 Multi Purpose Quick Freezing Device, Vacuum Device Inc., Mito, Ibaraki, Japan). The pair of grids was transferred, detached in liquid nitrogen, and immersed quickly into 2% OA solution and cooled in the abovementioned freezing device. Then, samples were transferred from the biosafety facility and placed in a freezer at −85 °C for several days, over which time the temperature was gradually raised to room temperature. Then, the OA solution was discarded and the samples were washed with absolute acetone three times at room temperature.

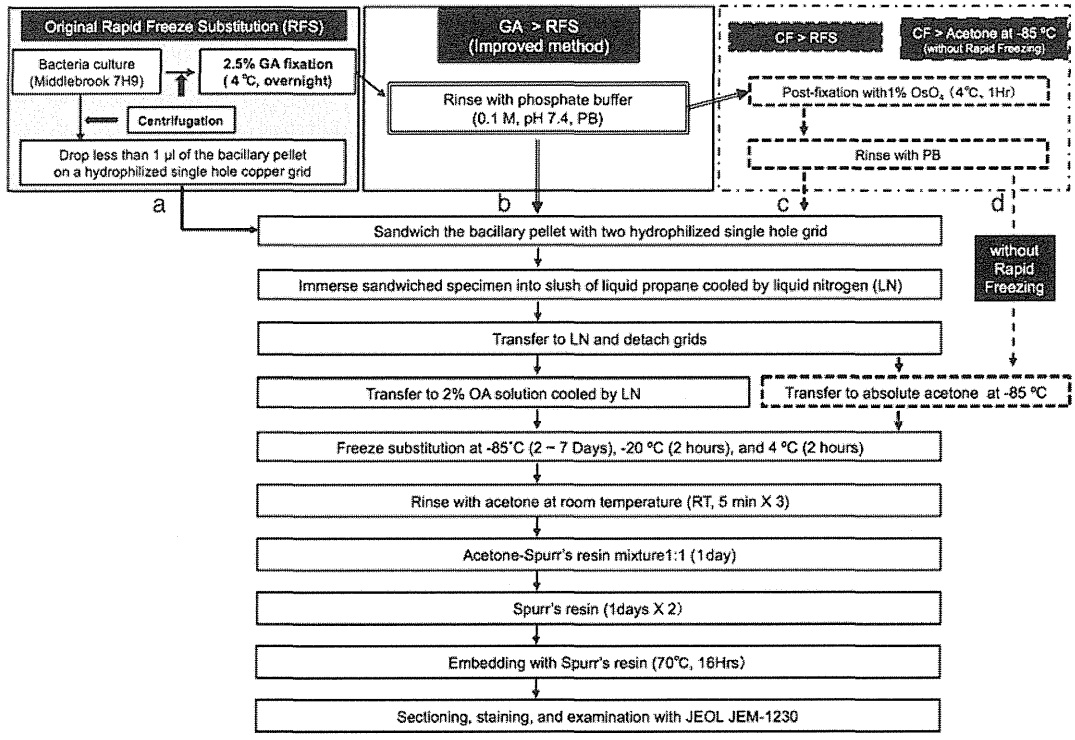

Fig. 1. Flowchart of the protocols for the four sample preparations used. (a) Original RFS, (b) GA > RFS, (c) CF > RFS, and (d) CF > acetone at −85 °C without rapid freezing. The steps contained in the shaded rectangle (top left) were performed in a type IIA biosafety cabinet at a biosafety level 3 facility. After fixation through exposure to 2% OA or 2.5% glutaraldehyde, the bacillary samples were transferred outside of the biosafety facility.

2.3. Transmission electron microscopy

The samples prepared with GA, CF, and RFS were embedded in Spurr's resin by using Leica/LKB Embedding Capsules Easy Molds. Ultrathin sections of average thickness 70 nm were sectioned with a Reichert Ultracut equipped with diamond knife, stained with uranyl acetate and lead citrate, and examined under a JEOL JEM-1230 electron microscope operated at 80 kV.

2.4. Image analysis and ribosome enumeration

Images were obtained through negative scanning using Adobe Photoshop Elements version 9 with CanoScan 8800F, and were saved as TIFF files and analyzed with ImageJ software (Rasband, 1997–2012). The number of ribosomes located in bacterial cytoplasm on scanned images was enumerated in a region of interest selected using a rectangular tool. Areas (μm^2) were measured using the ImageJ measure tool, and referenced against a scale bar on each negative. The number of ribosomes was converted and expressed as number per cubic micrometer (μm^3).

2.5. Statistics

Averages and standard deviations were calculated, and the randomization test for 2 independent samples was used to calculate statistical significance according to the following formula (Yamada et al., 2010, 2012)

$$t = \frac{x-y}{\sqrt{\left\{\sum_{i=1}^{n}(x_i-x)^2+\sum_{j=1}^{m}(y_j-y)^2\right\}/(n+m-2)}\ \sqrt{\frac{1}{n}+\frac{1}{m}}}.$$

Here, n and m represent the number of examined cells in two groups being compared, with average values x and y, respectively. Finally, the p value was determined from the obtained t value using a t distribution table.

3. Results and discussion

We have already reported the excellent preservation of the ultrastructure of mycobacterial cells attainable through RFS (Fig. 2, Yamada et al., 2010). Our original method allowed for RFS to be performed in a biosafety cabinet in a BSL 3 area using compact devices. However, it was impossible to use this method in laboratories without a safety cabinet in a BSL 3 area. Therefore, in this study we examined and developed a further application of this method for specimens pre-fixed with GA in order to allow the method to be used in conventional laboratories (Fig. 1). In this improved method, *M. tuberculosis* was cultured in a liquid medium for about 2 weeks and then fixed with 2.5% GA in PB in BSL 3 area, after which it was transferred to a conventional laboratory area and rinsed with PB. Then, after centrifugation, the highly concentrated bacillary pellet was subjected to RFS as in the original procedure. In the images obtained from the RFS samples that had undergone prior GA fixation (GA > RFS, Fig. 3), exquisite ultrastructure of tubercle bacilli was preserved intact and the image quality was comparable to the original RFS samples (RFS, Fig. 2). These images show clearly visible outer membranes, DNA fibers, and countable ribosomes in both the RFS and GA > RFS samples.

Furthermore, based on these results, we hypothesized that the preservation of exquisite ultrastructure obtained from the GA > RFS samples was attributable to cryofixation/substitution with OA at ultralow temperature, and not to substitution with acetone without OT at −85 °C. Therefore, we examined the ultrastructure of the samples fixed using GA and OT at 4 °C, equivalent to a conventional chemical fixation, prior to either RFS with absolute acetone at ultralow temperature (CF > RFS) or without rapid freezing (CF > freeze-substitution) in order to determine whether OT cryofixation or substitution with absolute acetone was the crucial process for the exquisite ultrastructure preservation in the GA > RFS-treated samples (Fig. 1). The images obtained from the samples for CF > RFS (Fig. 4a and b) and CF > freeze-substitution (Fig. 4c and d) were comparable to those obtained from the CF samples (Fig. 5); that is, the cytoplasm of the tubercle bacilli prepared by CF, CF > RFS, or CF > freeze-substitution was apparently constituted of two compartments with different electron density.

We demonstrated that this procedure can provide excellent images of tubercle bacilli ultrastructure. In this study, we improved our original method to enable most of the steps to be performed in a conventional laboratory following GA fixation of the virulent tubercle bacilli in a biosafety area. This improved method also provides excellent images of the ultrastructure comparable to that of the original RFS method. We demonstrated two important facts: first, that pre-fixation of the samples with GA did not degrade the final ultrastructures; second, that rapid freezing followed by cryofixation and substitution at ultralow temperature with OA is crucial for preserving the ultrastructure following pre-fixation with GA. Furthermore, it is revealed that cryofixation and substitution at ultralow temperature are indivisible steps and one cannot take the place of the other.

Although several studies have reported freeze-substitution following GA or CF, a few drew attention to the usefulness of the method for preparation of microbiological samples (Grief et al., 1994; Inoue, 1995; Sato et al., 1999; Yamaguchi et al., 2011) while fewer still reported examinations involving pathogenic organisms, such as pathogenic fungi, *Exophiala dermatitidis* and *Cryptococcus neoformans* (Yamaguchi et al., 2005). Furthermore, Couture-Tosi et al. (2010) demonstrated that GA

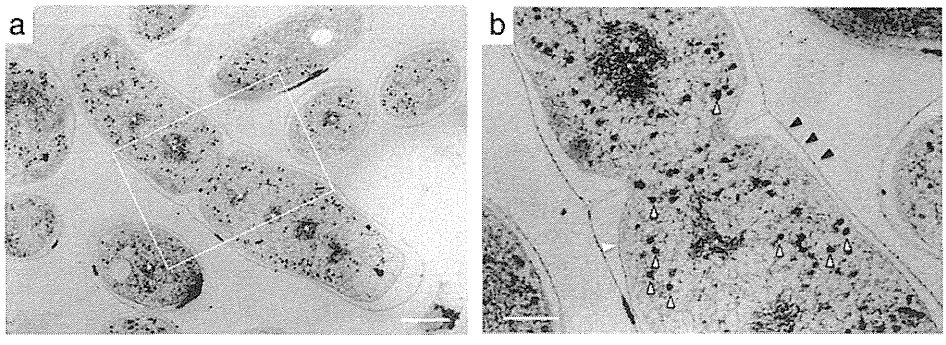

Fig. 2. TEM images of tubercle bacilli during cell division obtained from original RFS preparation. (a) is a low magnification image and (b) a higher magnification image of the indicated area in A, where the septum is clearly visible. Black arrowheads indicate outer membrane, white arrowheads indicate plasma membrane, white arrowheads outlined in black indicate ribosomes, and white asterisks indicate DNA fibers. Scale bars are 200 nm (a) and 100 nm (b).

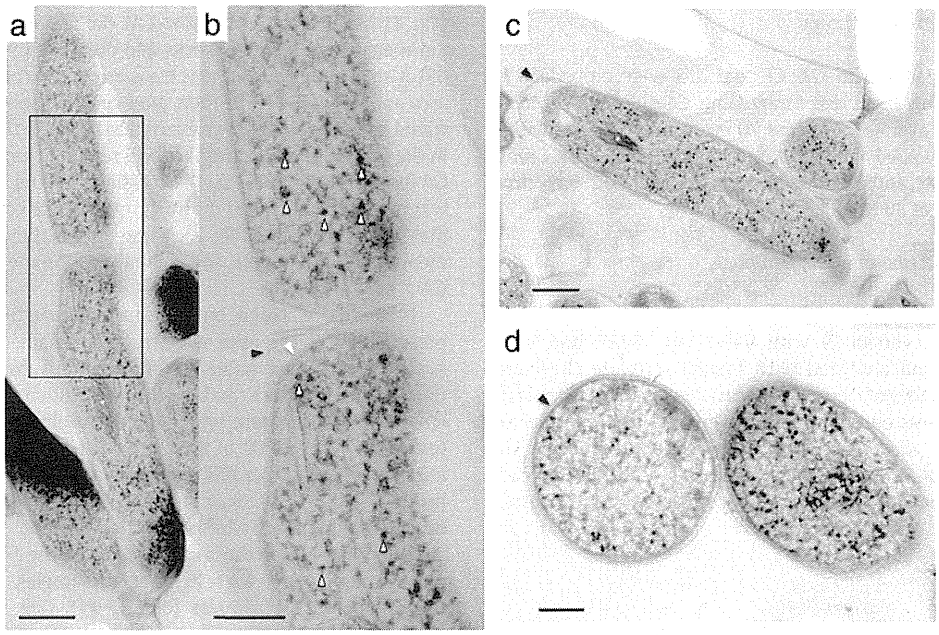

Fig. 3. TEM images of the tubercle bacilli during cell division obtained from GA > RFS preparation. (a) is a low magnification image and (b) a higher magnification image of the indicated area in (a), where the septum is clearly visible. (c) is another image of the longitudinal plane and (d) a cross-sectional image. Black arrowheads indicate outer membrane, white arrowheads indicate plasma membrane, white arrowheads outlined in black indicate ribosomes, and white asterisks indicate DNA fibers. Scale bars are 200 nm (a and c) and 100 nm (b and d).

pre-fixation was not associated with morphological changes in *Bacillus antracis* CEMOVIS samples, and our observations are in agreement with their finding.

Furthermore, Bleck et al. (2010) reported the results of a comparison between several preparation methods for transmission electron microscopy samples using *Mycobacterium smegmatis*, including classical chemical fixation, CEMOVIS, high-pressure freezing, and the Tokuyasu method. They concluded that CEMOVIS was the "gold standard" for cell imaging, with excellent preservation of intact cell ultrastructure. However, the sample used in their report was the nonpathogenic mycobacteria *M. smegmatis*, and GA > RFS preparation was not examined. Therefore, the present study is the first to demonstrate that GA > RFS of tubercle bacilli done in a conventional laboratory following GA fixation is able to preserve exquisite ultrastructure to a comparable extent as RFS, which must be performed entirely in a BSL 3 area when GA fixation is not performed.

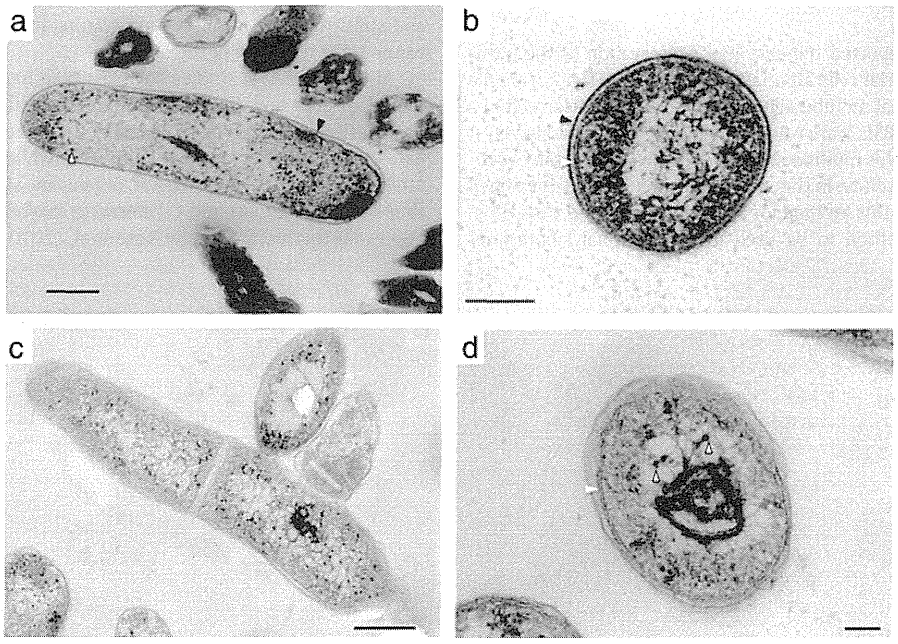

Fig. 4. TEM images of the tubercle bacilli obtained from CF > RFS preparation (a and b) and CF > acetone freeze-substitution at −85 °C (c and d). (a) and (c) are longitudinal images, and (b) and (d) cross-sectional images. Black arrowheads indicate outer membrane, white arrowheads indicate plasma membrane, and white arrowheads outlined in black indicate ribosomes. Scale bars are 200 nm (a and c), 100 nm (b), and 50 nm (d).

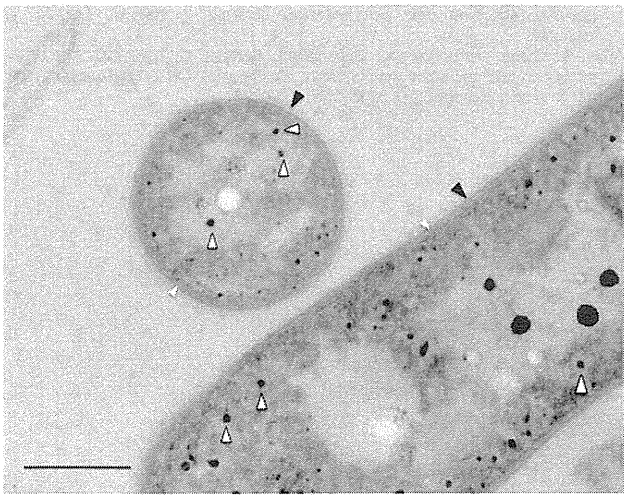

Fig. 5. TEM image of the tubercle bacilli obtained from CF preparation. Black arrowheads indicate outer membrane, white arrowheads indicate plasma membrane, and white arrowheads outlined in black indicate ribosomes. Scale bar is 200 nm.

In addition to comparing the images obtained from these preparation methods, we measured and compared the number of ribosomes observed in the samples prepared by GA > RFS, RFS, and CF. As shown in Fig. 6, the ribosome numbers enumerated on the images of the respective samples were 6987.8 ± 2181.0/μm^3, 6888.9 ± 1799.3/μm^3, and 5018.7 ± 2511.3/μm^3. The number of ribosomes detected in the samples prepared using GA > RFS and RFS was significantly higher than that found in the CF sample ($p = 0.04$ and $p = 0.05$, respectively), whereas there was no significant difference in ribosome number between GA > RFS and RFS ($p = 0.9$).

Previous studies reported the ribosomal density in *Mycobacterium bovis* BCG, calculated based on the quantitative relationships observed between specific growth rates of cells and their macromolecular compositions, as approximately 4000 ribosomes/μm^3 (=fl) (Comolli et al., 2009; Cox, 2003, 2004). Our enumeration of ribosomes based on TEM image examination described above was similar to these previous results, indicating that both our original and improved RFS methods can preserve the exquisite ultrastructure of tubercle bacilli well.

The improved RFS method would be extremely valuable to prepare specimens of viable but unculturable microbiological materials or clinical isolates of MDR- or XDR-TB which cannot be easily transferred from conventional laboratories to laboratories where RFS can be performed. Because, in this report, we could demonstrate the localization and density of ribosomes, which are the target of antibiotics such as aminoglycosides, this method should contribute to elucidating the mechanisms that cause drug resistance and to localizing the site of interaction between drugs and their target molecules.

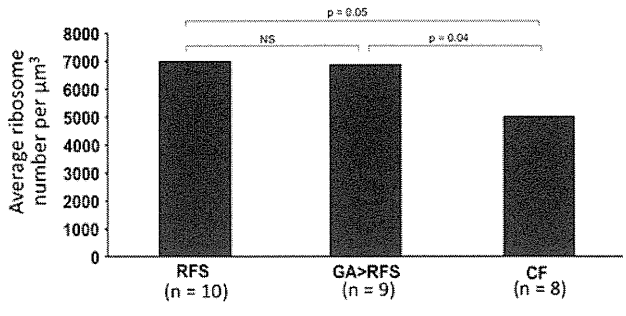

Fig. 6. Comparison of ribosome density between the preparation methods.

Acknowledgments

This work was supported by a Health Science Research grant from the Ministry of Health, Labour and Welfare of Japan (H24-SHINKO-IPPAN-011).

References

Aldridge, B.B., Fernandez-Suarez, M., Heller, D., Ambravaneswaran, V., Irimia, D., Toner, M., Fortune, S.M., 2012. Asymmetry and aging of mycobacterial cells lead to variable growth and antibiotic susceptibility. Science 335, 100–104.

Amako, K., Takade, A., Umeda, A., Matsuoka, M., Yoshida, S., Nakamura, M., 2003. Degradation process of *Mycobacterium leprae* cells in infected tissue examined by the freeze-substitution method in electron microscopy. Microbiol. Immunol. 47, 387–394.

Bleck, C.K., Merz, A., Gutierrez, M.G., Walther, P., Dubochet, J., Zuber, B., Griffiths, G., 2010. Comparison of different methods for thin section EM analysis of *Mycobacterium smegmatis*. J. Microsc. 237, 23–38.

Comolli, L.R., Baker, B.J., Downing, K.H., Siegerist, C.E., Banfield, J.F., 2009. Three-dimensional analysis of the structure and ecology of a novel, ultra-small archaeon. ISME J. 3, 159–167.

Couture-Tosi, E., Ranck, J.L., Haustant, G., Pehau-Arnaudet, G., Sachse, M., 2010. CEMOVIS on a pathogen: analysis of *Bacillus anthracis* spores. Biol. Cell. 102, 609–619.

Cox, R.A., 2003. Correlation of the rate of protein synthesis and the third power of the RNA: protein ratio in *Escherichia coli* and *Mycobacterium tuberculosis*. Microbiology 149, 729–737.

Cox, R.A., 2004. Quantitative relationships for specific growth rates and macromolecular compositions of *Mycobacterium tuberculosis*, *Streptomyces coelicolor* A3 (2) and *Escherichia coli* B/r: an integrative theoretical approach. Microbiology 150, 1413–1426.

Golchin, S.A., Stratford, J., Curry, R.J., McFadden, J., 2012. A microfluidic system for long-term time-lapse microscopy studies of mycobacteria. Tuberculosis 92, 489–496.

Grief, C., Nermut, M.V., Hockley, D.J., 1994. A morphological and immunolabelling study of freeze–substituted human ans simian immunodeficiency viruses. Micron 25, 119–128.

Hoffmann, C., Leis, A., Niederweis, M., Plitzko, J.M., Engelhardt, H., 2008. Disclosure of the mycobacterial outer membrane: cryo-electron tomography and vitreous sections reveal the lipid bilayer structure. Proc. Natl. Acad. Sci. U. S. A. 105, 3963–3967.

Hurbain, I., Sachse, M., 2011. The future is cold: cryo-preparation methods for transmission electron microscopy of cells. Biol. Cell. 103, 405–420.

Inoue, S., 1995. Possible continuity of subplasmalemmal cytoplasmic network with basement membrane cord network: ultrastructural study. J. Cell Sci. 108, 1971–1976.

Matias, V.R., Beveridge, T.J., 2006. Native cell wall organization shown by cryo-electron microscopy confirms the existence of a periplasmic space in *Staphylococcus aureus*. J. Bacteriol. 188, 1011–1021.

Paul, T.R., Beveridge, T.J., 1992. Reevaluation of envelope profiles and cytoplasmic ultrastructure of mycobacteria processed by conventional embedding and freeze-substitution protocols. J. Bacteriol. 174, 6508–6517.

Paul, T.R., Beveridge, T.J., 1994. Preservation of surface lipids and determination of ultrastructure of *Mycobacterium kansasii* by freeze-substitution. Infect. Immun. 62, 1542–1550.

Perez-Cruz, C., Carrion, O., Delgado, L., Martinez, G., Lopez-Iglesias, C., Mercade, E., 2013. New type of outer membrane vesicle produced by the Gram-negative bacterium *Shewanella vesiculosa* M7T: implications for DNA content. Appl. Environ. Microbiol. 79, 1874–1881.

Rasband, W.S., 1997–2012. ImageJ. U. S. National Institutes of Health, Bethesda, Maryland, USA (http://imagej.nih.gov/ij/).

Sato, M., Hasegawa, K., Shimada, S., Osumi, M., 1999. Effects of pressure stress on the fission yeast *Schizosaccharomyces pombe* cold-sensitive mutant nda3. FEMS Microbiol. Lett. 176, 31–38.

Takade, A., Umeda, A., Matsuoka, M., Yoshida, S., Nakamura, M., Amako, K., 2003. Comparative studies of the cell structures of *Mycobacterium leprae* and *M. tuberculosis* using the electron microscopy freeze-substitution technique. Microbiol. Immunol. 47, 265–270.

Wakamoto, Y., Dhar, N., Chait, R., Schneider, K., Signorino-Gelo, F., Leibler, S., McKinney, J.D., 2013. Dynamic persistence of antibiotic-stressed mycobacteria. Science 339, 91–95.

Yamada, H., Mitarai, S., Chikamatsu, K., Mizuno, K., Yamaguchi, M., 2010. Novel freeze-substitution electron microscopy provides new aspects of virulent *Mycobacterium tuberculosis* with visualization of the outer membrane and satisfying biosafety requirements. J. Microbiol. Methods 80, 14–18.

Yamada, H., Bhatt, A., Danev, R., Fujiwara, N., Maeda, S., Mitarai, S., Chikamatsu, K., Aono, A., Nitta, K., Jacobs Jr., W.R., Nagayama, K., 2012. Non-acid-fastness in *Mycobacterium tuberculosis* Δ*kasB* mutant correlates with the cell envelope electron density. Tuberculosis 92, 351–357.

Yamaguchi, M., Biswas, S.K., Suzuki, Y., Furukawa, H., Takeo, K., 2003. Three-dimensional reconstruction of a pathogenic yeast *Exophiala dermatitidis* cell by freeze-substitution and serial sectioning electron microscopy. FEMS Microbiol. Lett. 219, 17–21.

Yamaguchi, M., Ohkusu, M., Sameshima, M., Kawamoto, S., 2005. Safe specimen preparation for electron microscopy of pathogenic fungi by freeze-substitution after glutaraldehyde fixation. Jpn. J. Med. Mycol. 46, 187–192.

Yamaguchi, M., Okada, H., Namiki, Y., 2009. Smart specimen preparation for freeze substitution and serial ultrathin sectioning of yeast cells. J. Electron Microsc. 58, 261–266.
Yamaguchi, M., Namiki, Y., Okada, H., Uematsu, K., Tame, A., Maruyama, T., Kozuka, Y., 2011. Improved preservation of fine structure of deep-sea microorganisms by freeze-substitution after glutaraldehyde fixation. J. Electron Microsc. 60, 283–287.
Zuber, B., Chami, M., Houssin, C., Dubochet, J., Griffiths, G., Daffé, M., 2008. Direct visualization of the outer membrane of *Mycobacteria* and *Corynebacteria* in their native state. J. Bacteriol. 190, 5672–5680.

Chikamatsu et al. BMC Infectious Diseases 2014, 14:54
http://www.biomedcentral.com/1471-2334/14/54

BMC Infectious Diseases

RESEARCH ARTICLE Open Access

Comparative evaluation of three immunochromatographic identification tests for culture confirmation of *Mycobacterium tuberculosis* complex

Kinuyo Chikamatsu[1*], Akio Aono[1], Hiroyuki Yamada[1], Tetsuhiro Sugamoto[1], Tomoko Kato[1,2], Yuko Kazumi[1], Kiyoko Tamai[3], Hideji Yanagisawa[3] and Satoshi Mitarai[1,2]

Abstract

Background: The rapid identification of acid-fast bacilli recovered from patient specimens as *Mycobacterium tuberculosis* complex (MTC) is critically important for accurate diagnosis and treatment. A thin-layer immunochromatographic (TLC) assay using anti-MPB64 or anti-MPT64 monoclonal antibodies was developed to discriminate between MTC and non-tuberculosis mycobacteria (NTM). Capilia TB-Neo, which is the improved version of Capilia TB, is recently developed and needs to be evaluated.

Methods: Capilia TB-Neo was evaluated by using reference strains including 96 *Mycobacterium* species (4 MTC and 92 NTM) and 3 other bacterial genera, and clinical isolates (500 MTC and 90 NTM isolates). *M. tuberculosis* isolates tested negative by Capilia TB-Neo were sequenced for *mpt64* gene.

Results: Capilia TB-Neo showed 100% agreement to a subset of reference strains. Non-specific reaction to *M. marinum* was not observed. The sensitivity and specificity of Capilia TB-Neo to the clinical isolates were 99.4% (99.6% for *M. tuberculosis,* excluding *M. bovis* BCG) for clinical MTC isolates and 100% for NTM isolates tested, respectively. Two *M. tuberculosis* isolates tested negative by Capilia TB-Neo: one harbored a 63-bp deletion in the *mpt64* gene and the other possessed a 3,659-bp deletion from Rv1977 to Rv1981c, a region including the entire *mpt64* gene.

Conclusions: Capilia TB-Neo is a simple, rapid and highly sensitive test for identifying MTC, and showed better specificity than Capilia TB. However, Capilia TB-Neo still showed false-negative results with *mpt64* mutations. The limitation should be recognized for clinical use.

Keywords: Capilia TB-Neo, *Mycobacterium tuberculosis* complex identification, *mpt64* gene

Background

Tuberculosis remains a major threat to global health, and therefore, rapid identification of the causative *M. tuberculosis* complex (MTC) is critical. Liquid culture detection is now widely used for managing HIV-co-infected and drug-resistant tuberculosis, and liquid culture can improve the recovery of acid-fast bacilli and decreases the time to detection. However, because other non-tuberculosis mycobacterium (NTM) species may also grow, it is important to identify MTC from positive culture for rapid and appropriate management of tuberculosis.

Several methods are available to identify mycobacteria. Conventional biochemical tests are generally time-consuming [1,2] and not surely reproducible, while more recently developed techniques involving molecular biology [3-7] or high-performance liquid chromatographic analysis of mycolic acid [8] are accurate and rapid, but these require expensive devices. In contrast, immunochromatographic species identification tests, Capilia TB (TAUNS,

* Correspondence: chikamatsu@jata.or.jp
[1]Department of Mycobacterium Reference and Research, Research Institute of Tuberculosis, Japan Anti-Tuberculosis Association, Kiyose, Tokyo 204-8533, Japan
Full list of author information is available at the end of the article

Izunokuni, Japan), SD BIOLINE TB Ag MPT64 rapid (Standard Diagnostics, Inc., Korea) and BD MGIT™ TBc Identification Test (Becton, Dickinson and Company, USA) have been adopted as a cheap, rapid, and accurate alternative in clinical laboratories around the world [9-11]. However, false positives to *Mycobacterium marinum*, *Staphylococcus aureus* [9,12], and false negatives in MPB64 mutants [10,13] have occasionally been reported. Capilia TB-Neo (TAUNS, Izunokuni, Japan), an improved version of Capilia TB, has recently been developed to overcome these problems. In this study, we evaluated the performance of Capilia TB-Neo with reference strains and clinical isolates. Any false-negative MTC clinical isolate detected by Capilia TB-Neo were further investigated relative genes.

Methods

Reference strains and clinical isolates

Reference strains of 96 *Mycobacterium* species and subspecies (4 MTC and 92 NTM) and 3 other genera with acid-fastness (*Nocardia asteroids*, *Rhodococcus equi* and *Rhodococcus aichiense*) were used for the evaluation (Table 1). A total of 500 MTC and 90 NTM clinical isolates (10 *M. abscessus*, 4 *M. chelonae*, 13 *M. fortuitum*, 8 *M. gordonae*, 15 *M. avium* complex, 7 *M. intracellulare*, 3 *M. nonchromogenicum*, 5 *M. scrofulaceum*, 4 *M. xenopi*, 15 *M. kansasii*, 1 *M. gastri*, 2 *M. peregrinum*, 1 *M. intermedium*, 1 *M. szulgai*, and 1 *M. marinum*) were selected to provide a representative sample of the isolates available from Miroku Medical Laboratory Co., Ltd. (Saku, Japan) from 2009 to 2010, and the collection from the Ryoken survey in 2002 and 2007. The clinical isolates were collected from patients as a part of routine examination. No ethical approval was required for this type of laboratory based study only using isolates. Reference strains and clinical isolates were cultured with OADC-supplemented Middlebrook 7H9 broth (Becton, Dickinson and Company, USA) and 2% Ogawa medium (Kyokuto Pharmaceutical Industrial Co., Japan) at 37°C or 30°C.

Identification of mycobacteria

Mycobacterium species of the clinical isolates were identified using one or more of the following approaches: (i) the DNA or RNA amplification kits Cobas Amplicor PCR (Roche Diagnostics, Japan) and TRC Rapid (Tosoh Bioscience, Japan); (ii) the DNA-DNA hybridization DDH Mycobacteria Kit (Kyokuto Pharmaceutical Industrial Co., Japan); and (iii) 16S rRNA gene sequencing, supplementary [7]. The isolates identified as MTC were further examined by multiplex PCR analysis of *cfp32*, the region of difference (RD) 9, and RD12 according to the method of Nakajima et al. [14]. When MTC species other than *M. tuberculosis* sensu stricto were detected, they were further characterized with respect to RD1, RD4, RD7, and MiD3 [15]. If *M. bovis* Bacillus Calmette-Guerin (BCG) was identified, additional multiplex PCR analyses were performed to test for RD2, RD14, RD15, RD16, and *SenX3-RegX3* to distinguish sub-strains of BCG [16,17]. The multiplex PCR amplification was performed using a Type-it Microsatellite PCR Kit (QIAGEN, Japan). Each PCR reaction contained 1.0 μl of DNA template, 6.25 μl of Type-it multiplex PCR Master mix, 1.25 μl of Q-solution, 0.25 μl of each primer (10 pmol/μl) and an appropriate amount of molecular grade water for a total reaction volume of 13 μl. The thermal profile was as follows: (i) 95°C (5 min); (ii) 28 cycles of 95°C (0.5 min), 58 or 55°C (1.5 min), 72°C (0.5 min); and (iii) a final extension step at 68 or 60°C (10 or 30 min). The amplified products were analyzed by 3% agarose gel electrophoresis. The expected RD loci for each MTC species are summarized in Table 2.

Capilia TB-Neo, SD MPT64, and TBc ID

The validation of Capilia TB-Neo (TAUNS, Izunokuni, Japan) was conducted using the aforementioned reference strains as well as MTC and NTM clinical isolates. In addition, SD BIOLINE TB Ag MPT64 rapid (SD MPT64: Standard Diagnostics, Inc. Korea) and BD MGIT™ TBc Identification Test (TBc ID: Becton, Dickinson and Company, USA), detect MPT64 which is the same as MPB64, were tested using reference strains and NTM clinical isolates. Each test was performed according to the manufacturer's instructions. Briefly, clinical isolates growing on Ogawa medium were suspended in 1 ml of sterile distilled water, and the suspension subjected to the test. Similarly, positive liquid cultures of reference strains (McFarland No. 1 to 2) were directly subjected to each test. Positive test results were indicated by a red line in the test area after 15 min.

Sequencing of the *mpt64* gene

Any false-negative *M. tuberculosis* isolate detected by Capilia TB-Neo was further analyzed by sequencing *mpt64* and surrounding genes by using the primers listed in Table 2. Each PCR reaction contained 1.0 μl of DNA template, 12.5 μl of Type-it multiplex PCR Master mix, 2.5 μl of Q-solution, 0.5 μl of each primer (10 pmol/μl) and an appropriate amount of molecular grade water for a total reaction volume of 25 μl. The thermal profile was as follows: (i) 95°C (5 min); (ii) 30 cycles of 95°C (0.5 min), 62°C (1.5 min), 72°C (1 min); and (iii) final extension at 60°C (10 min). The amplified product was analyzed by 3% agarose gel electrophoresis and was purified using Mag Extractor (TOYOBO, Japan). The purified DNA products were subjected to direct sequencing using an ABI 377 automatic sequencer (Applied Biosystems, USA) and BigDye Terminator Cycle Sequencing v 3.1 (Applied Biosystems, USA), according to the manufacturer's instructions. DNA

Table 1 List of reference strains and the results of identification of MTC by using Capilia TB-Neo, SD MPT64, and TBc ID

Species	Strain	Capilia TB-Neo	SD MPT64	TBc ID	Species	Strain	Capilia TB-Neo	SD MPT64	TBc ID
M. tuberculosis H37Rv	ATCC27294	+	+	+	*M. interjectum*	ATCC51457	-	-	-
M. africanum	ATCC25420	+	+	+	*M. intermedium*	ATCC51848	-	-	-
M. bovis	ATCC19210	+	+	+	*M. intracellulare*	ATCC13950	-	-	-
M. microti	ATCC19422	+	+	+	*M. kansasii*	ATCC12478	-	-	-
M. abscessus	ATCC19977	-	-	-	*M. kubicae*	ATCC700732	-	-	-
M. acapulcensis	ATCC14473	-	-	-	*M. lactis*	ATCC27356	-	-	-
M. agri	ATCC27406	-	-	-	*M. lentiflavum*	ATCC51985	-	-	-
M. aichiense	ATCC27280	-	-	+	*M. madagascariense*	ATCC49865	-	-	-
M. alvei	ATCC51304	-	-	-	*M. malmoense*	ATCC29571	-	-	-
M. asiaticum	ATCC25276	-	-	-	*M. marinum*	ATCC00927	-	-	+
M. aurum	ATCC23366	-	-	-	*M. moriokaense*	ATCC43059	-	-	-
M. austroafricanum	ATCC33464	-	-	-	*M. mucogenicum*	ATCC49650	-	-	-
M. avium subsp. *avium*	ATCC25291	-	-	-	*M. neoaurum*	ATCC25795	-	-	-
M. avium subsp. *paratuberculosis*	ATCC19698	-	-	-	*M. nonchromogenicum*	ATCC19530	-	-	-
M. avium subsp. *"suis"*	ATCC19978	-	-	-	*M. novum*	ATCC19619	-	-	-
M. avium subsp. *silvaticum*	ATCC49884	-	-	-	*M. obuense*	ATCC27023	-	-	-
M. branderi	ATCC51789	-	-	-	*M. paraffinicum*	ATCC12670	-	-	-
M. brumae	ATCC51384	-	+	-	*M. parafortuitum*	ATCC19686	-	-	-
M. celatum	ATCC51131	-	-	-	*M. peregrinum*	ATCC14467	-	-	-
M. celatum II	ATCC51130	-	-	-	*M. petroleophilum*	ATCC21497	-	-	-
M. chelonae chemovar niacinogenes	ATCC35750	-	-	-	*M. phlei*	ATCC11758	-	-	-
M. chelonae subsp. *chelonae*	ATCC35752	-	-	-	*M. porcinum*	ATCC33776	-	-	-
M. chitae	ATCC19627	-	-	+	*M. poriferae*	ATCC35087	-	-	-
M. chlorophenolicum	ATCC49826	-	-	-	*M. pulveris*	ATCC35154	-	-	-
M. chubuense	ATCC27278	-	-	-	*M. rhodesiae*	ATCC27024	-	-	-
M. confluentis	ATCC49920	-	-	-	*M. scrofulaceum*	ATCC19981	-	-	-
M. conspicuum	ATCC700090	-	-	-	*M. senegalense*	ATCC35796	-	-	-
M. cookii	ATCC49103	-	-	-	*M. septicum*	ATCC700731	-	-	-
M. diernhoferi	ATCC19340	-	-	-	*M. shimoidei*	ATCC27962	-	-	-
M. duvalii	ATCC43910	-	-	-	*M. shinshuense*	ATCC33728	-	-	-
M. engbaekii	ATCC27353	-	-	-	*M. simiae*	ATCC25275	-	-	-
M. flavescens	ATCC14474	-	-	-	*M. smegmatis*	ATCC19420	-	-	-
M. fortuitum subsp. *acetamidolyticum*	ATCC35931	-	-	-	*M. smegmatis*	ATCC700084	-	-	-
M. fortuitum subsp. *fortuitum*	ATCC06841	-	-	-	*M. sphagni*	ATCC33027	-	-	-
M. fortuitum subsp. *fortuitum*	ATCC49403	-	-	-	*M. szulgai*	ATCC35799	-	-	-
M. gadium	ATCC27726	-	-	+	*M. terrae*	ATCC15755	-	-	-
M. gallinarum	ATCC19710	-	-	-	*M. terrae*	DSMZ43540	-	-	-
M. genavense	ATCC51234	-	-	-	*M. terrae*	DSMZ43541	-	-	-
M. gilvum	ATCC43909	-	-	-	*M. terrae*	DSMZ43542	-	-	-
M. goodii	ATCC700504	-	-	-	*M. thermoresistibile*	ATCC19527	-	-	-
M. gordonae	ATCC14470	-	-	-	*M. tokaiense*	ATCC27282	-	-	-
M. gordonae group B[19]	KK33-08	-	-	-	*M. triplex*	ATCC700071	-	-	-
M. gordonae group C[19]	KK33-53	-	-	-	*M. triviale*	ATCC23292	-	-	-

Table 1 List of reference strains and the results of identification of MTC by using Capilia TB-Neo, SD MPT64, and TBc ID *(Continued)*

M. gordonae group D[19]	KK33-46	-	-	-	*M. vaccae*	ATCC15483	-	-	-
M. haemophilum	ATCC29548	-	-	-	*M. valentiae*	ATCC29356	-	-	-
M. hassiacum	ATCC700660	-	-	-	*M. wolinskyi*	ATCC700010	-	-	-
M. heckeshornense	DSMZ44428	-	-	-	*M. xenopi*	ATCC19250	-	-	-
M. heidelbergense	ATCC51253	-	-	-	*Nocardia asteroides*	ATCC19247	-	-	-
M. hiberniae	ATCC49874	-	-	-	*Rhodococcus equi*	ATCC6939	-	-	-
					Rhodococcus aichiense	ATCC33611	-	-	-

sequences of *mpt64* from each isolate were compared with *M. tuberculosis* H37Rv by using Genetyx-win ver. 5.2 (Genetyx Co., Japan).

Results

Each of the three kits (Capilia TB-Neo, SD MPT64, and TBc ID) was tested using the 99 reference strains. Capilia TB-Neo correctly produced positive results for four MTC (*M. tuberculosis*, *M. africanum*, *M. bovis*, and *M. microti*) and negative results for 92 NTM and 3 non-mycobacterial species (other genera) with acid-fastness, while SD MPT64 and TBc ID generated several false positives (Table 1). The sensitivity and specificity of Capilia TB-Neo to reference strains were 100%.

Of the 500 MTC clinical isolates tested, 497 were identified as MTC by Capilia TB-Neo. The other 3 isolates that tested negative by using Capilia TB-Neo also tested negative by using SD MPT64 and TBc ID. All three kits produced negative results for all 90 NTM clinical isolates examined. Thus, The sensitivity and specificity of Capilia TB-Neo to the clinical isolates were 99.4% and 100%, respectively.

The multiplex PCR system identified 492 *M. tuberculosis* isolates out of 500. Five isolates, which were *cfp32*-, RD9-, RD4-, RD7-, and MiD3-positive, but RD12-negative, were initially identified as *M. canettii*. However, colonies of these isolates showed a consistent rough surface on solid medium, and subsequent sequencing of *hsp65* indicated that the isolates had the genotype of *M. tuberculosis* sensu stricto (data not shown). These isolates were collected from different areas of Japan. Consequently, 497 isolates were identified as *M. tuberculosis*. The remaining 3 isolates were deficient in RD1, RD4, RD7, RD9, and RD12, and therefore were identified as *M. bovis* BCG. Two of these isolates were confirmed as *M. bovis* BCG Tokyo based on the unique size of RD16, and the third isolate had the same RD pattern as BCG Connaught and BCG Montreal, as for RD2, RD14, RD15, RD16 and *SenX3-RegX3* (Figure 1). Among the 3 MTC isolates that tested negative by Capilia TB-Neo, 2 isolates were *M. tuberculosis* and the other was *M. bovis* BCG Connaught or BCG Montreal (Table 3).

Mutations in the *mpt64* gene were detected by sequencing two *M. tuberculosis* isolates with negative results by Capilia TB-Neo. One isolate had a deletion of 63 bp from nucleotides 196 to 258 (amino acids position 43 to 63), and the other had a deletion of 3,659 bp from nucleotide 874 in Rv1977 to nucleotide 905 in Rv1981c, which included the whole *mpt64* gene.

Discussion

In many industrialized countries, the ability to rapidly distinguish between MTC and NTM is critical in clinical practice. Indeed, the anti-tuberculosis drug resistance survey in Japan revealed that 19.3% of all clinical mycobacterial isolates are NTM [18], underscoring the importance of rapid and accurate detection of MTC from acid-fast bacillus-positive culture. The immunochromatographic assay kit for the identification of MTC is now widely used in many countries. Capilia TB-Neo is the improved version of Capilia TB, and has been subjected to few clinical evaluations. Here, we report good overall performance of the kit but with several limitations.

In this study, the sensitivity of Capilia TB-Neo was 99.4% to clinical MTC isolates or 99.6% excluding *M. bovis* BCG, while the specificity of the kit tested to clinical NTM isolates was 100%. However, the isolation of BCG could present a practical problem. The *M. bovis* BCG Tokyo strain is sporadically isolated in Japan as a complex of vaccination or bladder cancer therapy, and is identified as MTC with the kit [19]. Some BCG strains such as Connaught, Pasteur, and Tice lack RD2 including the *mpt64* gene, but RD2 is conserved in others such as Tokyo, Moreau, and Russia [16]. This issue should be properly addressed to avoid confusion. Although it is difficult to discriminate BCG Tokyo from MTC with *mpt64*/*mpb64*, their differentiation would be an important advance in the development of a future TLC product. The weak false-positive reaction to *M. marinum* that was reported using Capilia TB [12] was not observed in this study, and resulted in better specificity. The minimum

Table 2 Oligonucleotide primers used in PCR and direct sequencing

Target gene	Primer ID	Nucleotide sequence (5'-3')	Size (bp)	Ref. no.
MTC identification				
16S rRNA	285	GAGAGTTTGATCCTGGCTCAG	1028	7
	264	TGCACACAGGCCACAAGGGA		
	259	TTTCACGAACAACG GACAA	591	
cfp32	Rv0577F	ATGCCCAAGAGAAGCGAATACAGGCAA	786	14
	Rv0577R	CTATTGCTGCGGTGCGGGCTTCAA		
RD9	Rv2073cF	TCGCCGCTGCCAGATGAGTC	600	14
	Rv2073cR	TTTGGGAGCCGCCGGTGGTGATGA		
RD12	Rv3120F	GTCGGCGATAGACCATGAGTCCGTCTCCAT	404	14
	Rv3120R	GCGAAAAGTGGGCGGATGCCAG		
RD1	ET1	AAGCGGTTGCCGCCGACCGACC		15
	ET2	CTGGCTATATTCCTGGGCCCGG		
	ET3	GAGGCGATCTGGCGGTTTGGGG		
RD4	Rv1510F	GTGCGCTCCACCCAAATAGTTGC	1033	15
	Rv1510R	TGTCGACCTGGGGCACAAATCAGTC		
RD7	Rv1970F	GCGCAGCTGCCGGATGTCAAC	1116	15
	Rv1970R	CGCCGGCAGCCTCACGAAATG		
MiD3	IS1561F	GCTGGGTGGGCCCTGGAATACGTGAACTCT	530	15
	IS1561R	AACTGCTCACCCTGGCCACCACCATGGACT		
Distinguish sub-strains of BCG				
RD2	RD2l	CCAGATTCAAATGTCCGACC		16
	RD2r	GTGTCATAGGTGATTGGCTT		
RD14	RD14l	CAGGGTTGAAGGAATGCGTGTC		16
	RD14r	CTGGTACACCTGGGGAATCTGG		
RD15	RD8l	ACTCCTAGCTTTGCTGTGCGCT		16
	RD8r	GTACTGCGGGATTTGCAGGTTC		
RD16	RD16nf	ACATTGGGAAATCGCTGCTGTTG		17
	RD16nr	GGCTGGTGTTTCGTCACTTC		
SenX3-RegX3	C3	GCGCGAGAGCCCGAACTGC		16
	C5	GCGCAGCAGAAACGTCAGC		
Sequencing				
mpt64 (Rv1980c)	mpb64W-F	ACTCAGATATCGCGGCAATC	1061	this study
	mpb64W-R	CGATCACCTCACCTGGAGTT		
Rv1977	Rv1977F	GTTTCCCGAGATCAGCTCAA	348	this study
	Rv1977R	ATCTCGTCGTGTGTCACCAG		
Rv1981c	Rv1981F	GATCGAATGCAGGCTGGTAT	399	this study
	Rv1981R	ACTACTACCGCGGTGACGAC		

detection concentration of *M. tuberculosis* for Capilia TB-Neo was 10^5 CFU/ml (data not shown), which was one-tenth than that for the previous kit. There was a report that Cpilia TB-Neo was higher sensitivity than Capilia TB [20]. In summary, the overall performance of Capilia TB-Neo was better than Capilia TB in both sensitivity and specificity.

SD MPT64 and TBc ID were also tested with reference strains. Both SD MPT64 and TBc ID showed false-positive results against several NTM strains in this study. Kodama et al. [12] reported that no *M. marinum* strains grown on 2% Ogawa medium tested positive by using the Capilia TB, while all strains grown on 3 kinds of liquid medium, MGIT (Becton Dickinson, Japan), KRD

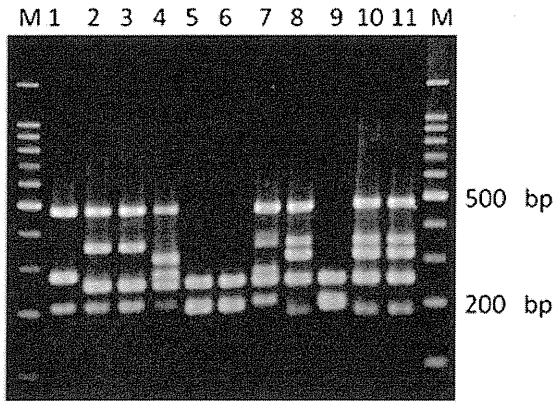

Figure 1 Multiplex PCR analysis of *Mycobacterium bovis* BCG sub-strains and clinical isolates. 1: BCG Pasteur (ATCC35734), 2: BCG Glaxo (ATCC35741), 3: BCG Copenhagen (ATCC27290), 4: BCG Russian (ATCC35740), 5: BCG Montreal (ATCC35735), 6: BCG Connaught (ATCC35745), 7: BCG Danish, 8: BCG Tokyo, 9: Sample 421, 10: Sample 467, 11: Sample 475, M: Size marker.

medium (Japan BCG Laboratory, Japan) and Myco Acid (Kyokuto Pharmaceutical Industrial Co. Ltd., Japan), eventually displayed a positive reaction that intensified with time. Kodama et al. speculated that nonspecific antigen which could make complex with anti-MPB64 antibody may be produced in liquid mediums, but not on solid medium. Considering the effect of liquid culture, the original bacterial suspensions giving false-positive results, that were prepared from liquid and solid culture, were then re-tested before and after 10-fold dilution. Interestingly, none of these diluted strains tested positive in these kits, but bacterial concentrations were high enough for positive results in case of MTC. These results implied that a high concentration of bacterial antigens could induce non-specific reactions in SD MPT64 and TBc ID. The manufacturer's instructions for the TBc ID indicate that this kit may be used up to 10 days after a positive MGIT alarm. This non-specific reaction should be properly addressed in clinical practice, and the users should perform morphological characterization with a microscope to identify cord formation.

Several mutations in the *mpt64* gene produce a negative test result for *M. tuberculosis* isolates in the TLC assay using anti-MPB64 monoclonal antibodies. To date, these include a 63-bp deletion from nucleotide 196, a 1-bp deletion from nucleotide 266, a point mutation at position 388 or 402, *IS6110* insertion mutation at position 177 or 501, a 176-bp deletion from nucleotide 512, and a 1-bp insertion at position 287 [10,13,21]. In our study, 2 *M. tuberculosis* isolates gave false-negative results by using the Capilia TB-Neo, SD MPT64, and TBc ID. One isolate had a deletion of 63 bp from nucleotide 196 in the *mpt64* gene as reported previously, and the other isolate possessed a 3,659-bp deletion from nucleotide 874 in Rv1977 to 905 in Rv1981c, including the whole *mpt64* gene. To the best of our knowledge, this is the first report of a large deletion in *mpt64*. A transposon site hybridization (TraSH) study [22] indicated that *mpt64* is not essential for infection or *in vitro* growth of *M. tuberculosis*. This large deletion mutant supported the finding.

In summary, the TLC assay detecting MPB64 or MPT64 can be applied to specimens prepared from liquid and solid culture. It does not need special reagents, instruments, or complex techniques. Capilia TB-Neo tested in this study showed excellent sensitivity with perfect specificity.

Conclusions

Capilia TB-Neo showed high sensitivity and specificity with clinical mycobacterial isolates, and 100% specificity to reference strains. However, 2 *M. tuberculosis* isolates were tested negative by Capilia TB-Neo because of mutations in the *mpt64* gene, and positive to certain BCG sub-strain. This study, therefore, serves to emphasize the importance of careful use of the kit and the complementary techniques such as morphological identification.

Table 3 Results of PCR detection and Capilia TB-Neo of MTC with clinical isolates

Species interpretation (Number of isolates)	Banding pattern							Capilia TB-Neo	%
	cfp32	RD9	RD12	RD4	RD7	MiD3	RD1		
M. tuberculosis (490)	+	+	+	NT	NT	NT	NT	+	98.0
M. tuberculosis (2)	+	+	+	NT	NT	NT	NT	-	0.4
"M. canettii" (5)[a]	+	+	-	+	+	+	+	+	1.0
M. bovis BCG Tokyo (2)[b]	+	-	-	-	-	+	-	+	0.4
M. bovis BCG Connaught (1)[c]	+	-	-	-	-	+	-	-	0.2

[a]Confirmed to be *M. tuberculosis* by *hsp65* sequencing and morphology, [b]Confirmed by contracted RD16, [c]Confirmed by absence of RD2 and RD15, and contracted *SenX3-RegX3*, NT: Not tested.

Competing interests
The authors declare that they have no competing interests.

Authors' contributions
KC carried out the TLC assays, molecular genetic studies, sequence alignment and drafted the manuscript. AA, HY, TS, and TK cultured clinical isolates. HY helped to draft the manuscript. YK prepared reference strains. KT and HY collected clinical isolates. SM was responsible for planning the study. All authors read and approved the final manuscript.

Acknowledgements
We thank TAUNS Co, Ltd (Izunokuni, Japan) for providing the Capilia TB-Neo, SD MPT64, and TBc ID.

Author details
[1]Department of Mycobacterium Reference and Research, Research Institute of Tuberculosis, Japan Anti-Tuberculosis Association, Kiyose, Tokyo 204-8533, Japan. [2]Department of Basic Mycobacteriosis, Nagasaki University Graduate School of Biomedical Sciences, Nagasaki 852-8501, Japan. [3]Miroku Medical Laboratory Company Limited, 659-2 Innai, Saku, Nagano 384-2201, Japan.

Received: 21 August 2013 Accepted: 27 January 2014
Published: 1 February 2014

References

1. Public Health Mycobacteriology: **A guide for the level III laboratory.** In *Identification Test Techniques: Department of Health and Human Services.* Atran: Public Health Service. CDC; 1985.
2. Rastogi N, Goh KS, David HL: **Selective inhibition of the *Mycobacterium tuberculosis* complex by *p*-nitro-a-acetylamino-b-hydroxypropiophenone (NAP) and *p*-nitrobenzoic acid (PNB) used in 7H11 agar medium.** *Res Microbiol* 1989, **140**:419–423.
3. Goto M, Oka S, Okuzumi K, Kimura S, Shimada K: **Evaluation of acridinium ester-labeled DNA probes for identification of *Mycobacterium tuberculosis* and *Mycobacterium avium-Mycobacterium intracellulare* complex in culture.** *J Clin Microbiol* 1991, **29**:2473–2476.
4. Ioannidis P, Papaventsis D, Karabela S, Nikolaou S, Panagi M, Raftopoulou E, Konstantinidou E, Marinou I, Kanavaki S: **Cepheid GeneXpert MTB/RIF Assay for *Mycobacterium tuberculosis* detection and rifampin resistance identification in patients with substantial clinical indications of tuberculosis and smear-negative microscopy results.** *J Clin Microbiol* 2011, **49**:3068–3070.
5. Mitarai S, Okumura M, Toyota E, Yoshiyama T, Aono A, Sejimo A, Azuma Y, Sugahara K, Nagasawa T, Nagayama N, Yamane A, Yano R, Kokuto H, Morimoto K, Ueyama M, Kubota M, Yi R, Ogata H, Kudoh S, Mori T: **Evaluation of a simple loop-mediated isothermal amplification test kit for the diagnosis of tuberculosis.** *Int J Tuberc Lung Dis* 2011, **15**:1211–1217.
6. Richter E, Rüsch-Gerdes S, Hillemann D: **Evaluation of the genotype Mycobacterium assay for identification of Mycobacterial species from cultures.** *J Clin Microbiol* 2006, **44**:1769–1775.
7. Springer B, Stockman L, Teschner KD, Roberts G, Bottger EC: **Two-laboratory collaborative study on identification of Mycobacteria: molecular versus phenotypic methods.** *J Clin Microbiol* 1996, **34**:296–303.
8. Standardized Method for HPLC Identification of Mycobacteria: **Department of Health and Human Services.** Atranta: Public Health Service CDC; 1996.
9. Abe C, Hirano K, Tomiyama T: **Simple and rapid identification of *Mycobacterium tuberculosis* complex by immunochromatographic assay using anti-MPB64 monoclonal antibodies.** *J Clin Microbiol* 1999, **37**:3693–3697.
10. Hillemann D, Rüsch-Gerdes S, Richter E: **Application of the Capilia TB assay for culture confirmation of *Mycobacterium tuberculosis* complex isolates.** *Int J Tuberc Lung Dis* 2005, **9**:1409–1411.
11. Muyoyeta M, de Haas PE, Mueller DH, van Helden PD, Mwenge L, Schaap A, Kruger C, Gey van Pittius NC, Lawrence K, Beyers N, Godfrey-Faussett P, Ayles H: **Evaluation of the Capilia TB assay for culture confirmation of Mycobacterium tuberculosis infections in Zambia and South Africa.** *J Clin Microbiol* 2010, **48**:3773–3775.
12. Kodama A, Saito H: **Evaluation of CapiliaTB for identification of *Mycobacterium tuberculosis* complex, with special reference to the culture medium.** *Jpn Society Clin Microbiol (in Japanese)* 2007, **17**:109–118.
13. Hirano K, Aono A, Takahashi M, Abe C: **Mutations including IS*6110* insertion in the gene encoding the MPB64 protein of Capilia TB negative *Mycobacterium tuberculosis* isolates.** *J Clin Microbiol* 2004, **42**:390–392.
14. Nakajima C, Rahim Z, Fukushima Y, Sugawara I, Van der Zanden AGM, Tamaru A, Suzuki Y: **Identification of *Mycobacterium tuberculosis* clinical isolates in Bangladesh by a species distinguishable multiplex PCR.** *BMC Infect Dis* 2010, **10**:118.
15. Huard RC, Fabre M, de Haas P, Lazzarini LC, van Soolingen D, Cousins D, Ho JL: **Novel genetic polymorphisms that further delineate the phylogeny of the *Mycobacterium tuberculosis* complex.** *J Bacteriology* 2006, **188**:4271–4287.
16. Bedwell J, Kario SK, Behr MA, Bygraves JA: **Identification of substrains of BCG vaccine using multiplex PCR.** *Vaccine* 2001, **19**:2146–2151.
17. Seki M, Sato A, Honda I, Yamazaki T, Yano I, Koyama A, Toida I: **Modified multiplex PCR for identification of Bacillus Calmette-Guerin substrain Tokyo among clinical isolates.** *Vaccine* 2005, **23**:3099–3102.
18. Tuberculosis Research Committee (Ryoken): **Drug-resistant *Mycobacterium tuberculosis* in Japan: a nationwide survey, 2002.** *Int J Tuberc Lung Dis* 2007, **11**:1129–1135.
19. Morokuma Y, Uchida Y, Karashima T, Fujise M, Imamura S, Kayamori Y, Kang DC: **Identification of Mycobacterium tuberculosis Complex Strains in Kyushu University Hospital.** *J J Clin Microbiol (in Japanese)* 2008, **18**:177–182.
20. Muyoyeta M, Mwanza WC, Kasese N, Cheeba-Lengwe M, Moyo M, Kaluba-Milimo D, Ayles H: **Sensitivity, specificity, and reproducibility of the Capilia TB-Neo assay.** *J Clin Microbiol* 2013, **51**:4237–4239.
21. Yu MC, Chen HY, Wu MH, Huang WL, Kuo YM, Yu FL, Jou R: **Evaluation of the rapid MGIT TBc identification test for culture confirmation of *Mycobacterium tuberculosis* complex strain detection.** *J Clin Microbiol* 2011, **49**:802–807.
22. Sassetti CM, Boyd DH, Rubin EJ: **Genes required for mycobacterial growth defined by high density mutagenesis.** *Mol Microbiol* 2003, **48**:77–84.

doi:10.1186/1471-2334-14-54
Cite this article as: Chikamatsu *et al.*: Comparative evaluation of three immunochromatographic identification tests for culture confirmation of *Mycobacterium tuberculosis* complex. *BMC Infectious Diseases* 2014 **14**:54.

Pathogens and Disease ISSN 2049-632X

RESEARCH ARTICLE

Mycobacterium tuberculosis escapes from the phagosomes of infected human osteoclasts reprograms osteoclast development via dysregulation of cytokines and chemokines

Akiyoshi Hoshino[1,2,3], Sanshiro Hanada[3], Hiroyuki Yamada[4], Shinji Mii[2], Masahide Takahashi[2], Satoshi Mitarai[4], Kenji Yamamoto[3] & Yoshinobu Manome[1]

1 Department of Molecular Cell Biology, Institute of DNA Medicine, Jikei University School of Medicine, Tokyo, Japan
2 Department of Pathology, Nagoya University Graduate School of Medicine, Nagoya, Japan
3 Vice Director's Lab, Research Institute, National Center for Global Health and Medicine, Tokyo, Japan
4 Department of Mycobacterium Reference and Research, Research Institute of Tuberculosis, Japan Anti-Tuberculosis Association, Tokyo, Japan

In the context of spinal tuberculosis a study of the inflammatory responses of human multinucleated osteoclasts infected with virulent *Mtb* is of interest. Intracellular *Mtb* infection resulted in the rapid growth of *Mtb* and production of proinflammatory cytokines. In contrast, highly-fused multinucleated osteoclasts incapacitated the production of these cytokines, *Mtb* escaped from the endosome/phagosome, and led to a different pattern of osteoclast activation with the production of a set of chemokines. These findings indicate that intracellular *Mtb* infection in multinuclear osteoclasts reprograms osteoclast development via the dysregulation of cytokines and chemokines.

Keywords
chemokines; chemokine receptors; host defense; inflammation; *Mycobacterium tuberculosis*; osteoclast.

Correspondence
Kenji Yamamoto, Vice Director's Lab, Research Institute, National Center for Global Health and Medicine. Toyama 1-21-1, Shinjuku-ku Tokyo 162-8655, Japan.
Tel.: +81-3-3202-7181 ext2856
fax: +81-3-3202-7364
e-mail: ykenji@hosp.ncgm.go.jp

Received 15 February 2013; revised 3 July 2013; accepted 30 July 2013.

doi:10.1111/2049-632X.12082

Editor: Patrick Brennan

Abstract

Spinal tuberculosis is a condition characterized by massive resorption of the spinal vertebrae due to the infection with *Mycobacterium tuberculosis* (*Mtb*). However, the pathogenesis of spinal tuberculosis has not been established because it was almost completely eradicated by the establishment of antibiotic treatment in the mid-20th century. In this study, we investigated the inflammatory responses of human multinucleated osteoclasts infected with virulent *Mtb* strain. We found that the intracellular *Mtb* infection of multinuclear osteoclasts resulted in the rapid growth of *Mtb* and an osteolytic response, rather than inflammation. In response to *Mtb* infection, the mononuclear osteoclast precursors produced proinflammatory cytokines including tumor necrosis factor (TNF)-α, an intrinsic characteristic they share with macrophages. In contrast, highly fused multinucleated osteoclasts incapacitated the production of these cytokines. Instead, the intracellular *Mtb* inside multinuclear osteoclasts escaped from the endosome/phagosome, leading to a different pattern of osteoclast activation, with the production of chemokines such as CCL5, CCL17, CCL20, CCL22, CCL24, and CCL25. Moreover, intracellular infection with an avirulent *Mtb* strain resulted in diminished production of these chemokines. These findings indicate that intracellular *Mtb* infection in multinuclear osteoclasts reprograms osteoclast development via the dysregulation of cytokines and chemokines.

Introduction

Inflammatory bone diseases are characterized by the infiltration of immune cells, including lymphocytes, monocytes, polymorphonuclear leukocytes, and even activated osteoclasts. Spinal tuberculosis (also called Pott's disease) is defined as a chronic inflammatory destruction of spinal bones, mainly induced by the mycobacterial infection of the spinal cavity, and is believed to be initiated by the abnormal activation of osteoclasts in the bone tissue, which leads to inflammatory bone destruction (Haynes, 2004), fracture, and collapse of the vertebrae, resulting in massive kyphotic deformities. Finally, the spinal canal may become narrower because of abscesses, granulation tissue or direct dural invasion, leading to spinal cord compression and neurological deficits.

The mortality from tuberculosis has decreased dramatically in developed countries following the introduction of effective chemotherapeutic agents in the mid-20th century, including isoniazid, rifampicin, pyrazinamide, streptomycin,

and ethambutol, before the molecular biology-based pathological mechanism of the disease had been completely revealed. However, *Mycobacterium tuberculosis* (*Mtb*) now affects one-third of the world population, and causes almost 2 million deaths per year; 30% of new cases can be found in India, China, Africa, and South America (WHO, 2012). In addition, current treatments are becoming obsolete because of the emergence of drug-resistant strains of *Mtb*. Thus, the development of a new, improved vaccine and/or new drugs that tackle the emergence of antibiotic resistance are sorely needed.

There is a question remaining as to whether osteoclastic activation and differentiation are facilitated at the inflammatory sites of spinal tuberculosis. It is well known that activated osteoclasts play an important role in inflammatory bone destruction, such as that occurring due to rheumatoid arthritis and inflammatory osteolysis. Similarly, spinal tuberculosis is believed to develop as a result of the activation of osteoclasts in bone tissue in response to *Mtb* infection, as an enormous amount of multinuclear osteoclast-like cells surrounding granulomatous caseous necrosis were observed around destroyed bones in a histological analysis. In fact, the development of spinal tuberculosis seems to be related to the infiltration of inflammatory immune cells into the bone tissue. However, there are no data available concerning whether *Mtb* directly infects the multinuclear osteoclasts intracellularly. Thus, we assumed that the source of *Mtb*-activated osteoclasts in spinal tuberculosis was as follows; (1) abnormal activation of *Mtb*-infected macrophages or their precursors in the inflammatory sites following a local infection, and subsequent activation of the RANK-RANKL axis, (2) abnormal induction and extravasation of *Mtb*-infected mononuclear osteoclast precursors from circulating cells into the inflammatory sites due to systemic infection, resulting in abnormal activation, and (3) unexpected pathogenic activation and reprogramming of multinuclear osteoclasts resident in the tissue in response to *Mtb* infection, followed by the dysregulation of cytokines and chemokines, causing the pathological destruction of the bone tissue.

Generally, proinflammatory cytokines, such as tumor necrosis facter (TNF)-α, interleukin (IL)-1β, and IL-6, are produced by macrophages in response to bacterial infection; proinflammatory cytokines also promote osteoclastogenesis (Boyle *et al.*, 2003). In the case of rheumatoid arthritis, the RANK-RANKL axis plays a principal role in the promotion of osteoclast differentiation. This is because the higher expression of RANKL in synovial fibroblasts, which is strongly induced by the autoreactive T cells that infiltrated into the synovial tissue, directs pathological osteoclast differentiation via the production of proinflammatory cytokines (Takayanagi *et al.*, 2000a, b). Bacterial pathogens surged RANKL via Toll-like receptor (TLR)-mediated signaling (Kikuchi *et al.*, 2001; Jiang *et al.*, 2002; Suda *et al.*, 2002); however, several reports suggested that proinflammatory cytokines (Boyle *et al.*, 2003) and several bacterial molecules act as promoters of osteoclastogenesis via the enhancement of RANKL through several TLRs (Kikuchi *et al.*, 2001; Jiang *et al.*, 2002; Suda *et al.*, 2002), whereas other studies reported that bacterial stimulation suppressed the generation of osteoclast precursors (Takami *et al.*, 2002; Ji *et al.*, 2009). Thus, it is still not clear whether bacterial stimulation promotes osteoclastogenesis.

Recently, chemokines have been recognized to be major factors involved in osteolysis and pathological osteoclastogenesis (Oba *et al.*, 2005; Kim *et al.*, 2006). CCL3/MIP-1α induces ectopic osteoclastogenesis in osteolytic lesions of rheumatoid arthritis (Haringman *et al.*, 2006; Menu *et al.*, 2006) and multiple myeloma (Choi *et al.*, 2000; Han *et al.*, 2001; Haringman *et al.*, 2006), implying that CCL3 and its receptor CCR1 act as a crucial chemokine for communication between osteoclasts and osteoblasts (Hoshino *et al.*, 2010). The participation of other axes of chemokines–chemokine receptors such as CCL2-CCR2 axis (Kim *et al.*, 2006; Li *et al.*, 2007; Binder *et al.*, 2009), CCL5-CCR5 axis (Oba *et al.*, 2005; Menu *et al.*, 2006; Hoshino *et al.*, 2009), and CX3CL1-CX3CR1 axis (Saitoh *et al.*, 2007; Koizumi *et al.*, 2009; Hoshino *et al.*, 2013) also play roles in bone remodeling. Nowadays, some types of chemokines are responsible for pathological bone destruction through the regulation of osteoclasts and their precursor cells that are derived from common progenitor cells in bone marrow, thus suggesting that several chemokine antagonists provide a strong rationale for further development of the therapeutic targets of associated osteolytic bone disease such as multiple myeloma and rheumatoid arthritis (Oba *et al.*, 2005; Menu *et al.*, 2006; Dairaghi *et al.*, 2012). These findings are referenced in favor of therapeutic treatments targeting chemokines to prevent pathogenic bone resorption.

To clarify the pathological mechanism underlying the overactivation of osteoclasts observed in tuberculosis-related osteolytic lesions, we stimulated osteoclasts and their precursors with virulent living *Mtb* and investigated the expression profiles of chemokines specific for tuberculosis infection.

Materials and methods

Ethical guidelines for human studies

All human experiments were performed with the approval of the local ethics committees of the Research Institute of National Center for Global Health and Medicine (No. H21-785).

Cells, materials, and bacteria

Mycobacterium tuberculosis H37Rv virulent laboratory strain (ATCC 27294), *Mycobacterium tuberculosis* H37Ra avirulent strain (ATCC 25177), and *Mycobacterium bovis* BCG-Tokyo vaccine strain were cultured at exponential growth phase in Middlebrook 7H9 broth (BD, Sparks, MD) with ADC enrichment (BD) and 0.05% Tween 80 at 37 °C for 7–10 days. Lipopolysaccharide (LPS) from *Escherichia coli* O55B5 and peptidoglycan (PGN) from *Staphylococcus aureus* were purchased from Sigma Aldrich (St. Louis, MO)

and Fluka Chemical (St. Gallen, Switzerland), respectively. Recombinant human M-CSF and RANKL were purchased from R&D Systems Inc. (Minneapolis, MN). Normal human natural mononuclear osteoclast precursors cells (Poietics™ Osteoclast Precursor Cell System) were purchased from Lonza Walkersville, Inc. (Walkersville, MD) and maintained with osteoclast precursor cell basal medium in the presence of 10 ng mL^{-1} M-CSF (without RANKL) and used as mononuclear osteoclast precursors (precursor mononuclear cells; pMCs). The multinuclear osteoclasts were induced according to the manufacturer's instructions. Human peripheral blood monocytes were collected from a healthy volunteer, separated using CD11b MicroBeads (Miltenyi Biotec Inc., Bergisch Gladbach, Germany), and stored at –80 °C prior to use.

Osteoclast culture and intracellular *Mtb* infection

Mononuclear pMCs were cultured with osteoclast precursor cell basal medium (Lonza), and the culture medium was replaced every 3 days. The highly fused multinuclear osteoclasts (multinuclear osteoclasts; mOCs) were induced from mononuclear cells with 10 ng mL^{-1} M-CSF and 20 ng mL^{-1} RANKL for 5 days. Intracellular *Mtb* infection was performed by the co-culture of mononuclear pMCs and multinuclear mOCs (5×10^4 cells per well, 1 mL) with 0.5 μL of *Mtb* H37Rv broth (equivalent to 1.0×10^5 CFU per wells) for 24 h to minimize the influence of bacterial broth, and the excess bacteria were rinsed off with phosphate-buffered saline (PBS). The culture supernatants of stimulated osteoclasts were harvested, irradiated with UV-C (254-nm wavelength) for 30 s, and filtered with Ultrafree-FC® 0.1-μm membrane filters (Merck Millipore, Darmstadt, Germany) to remove living *Mtb*. For immunohistochemical staining, osteoclasts were fixed with 4% paraformaldehyde, permeabilized and stained with the indicated specific Abs or Alexa488-labeled phalloidin (Molecular Probes). The images were captured using an IX-81 fluorescent microscopy (Olympus Corp, Tokyo, Japan) equipped with a confocal microscopy DSU unit (Olympus) and analyzed by MetaMorph (Universal Imaging corporation, Molecular Devices, Downingtown, PA).

Ziehl–Neelsen staining

For acid-fast bacterial staining, the culture slides (LabTech® chamber slide system, Nunc-Nalgene™, Thermo Fisher Scientific, Waltham, MA) were fixed, stained with steps of 0.3% carbol-fuchsin solution, decolorization with a 3% hydrochloric acid/95% ethanol solution, and counterstaining with Löffrel's methylene blue. The slides were rinsed, allowed to dry, and examined under a binocular microscope with oil immersion.

Electron microscopic examination of infected osteoclasts

Osteoclasts cultured and infected with the *Mtb* H37Rv strain were fixed with 2.5% glutaraldehyde in 100 mM phosphate buffer (PB, pH7.4) for 1 h at 4 °C, rinsed three times with PB, and post-fixed with 1% osmium tetroxide. Then, the samples were dehydrated with a graded ethanol series, embedded with Spurr's resin and polymerized at 70 °C for 16 h. Ultrathin sections were cut, stained with uranyl acetate and lead citrate, and examined with a JEOL JEM-1230 microscope (Yamada *et al.*, 2001).

Real-time PCR analysis

A real-time quantitative PCR analysis was performed using an ABI 7700 sequence detector system with the purchased probe sets (Taqman® gene expression analysis system, Applied Biosystems, Foster City, CA). The sequences were amplified for 40 cycles under the following two-step parameters: denaturation at 95 °C for 15 s, annealing, and extension at 60 °C for 60 s. The relative gene expression levels were normalized by the expression of *GAPDH* by the $2^{-\Delta(Ct)}$ method.

Measurement of cytokines and chemokines, and TRAP activity

The production of chemokines was determined using DuoSet® ELISA kits (R&D systems) for CCL17, CCL20, CCL22, CCL24, and CCL25. The cytokines [TNF-α, IL-1β, IL-6, IL-8, and interferon (IFN)-γ] and chemokines (CCL2, CCL3, and CCL5) were measured using the human 27-plex multiple cytokine detection system (Bio-Rad Corp., Hercules, CA) according to the manufacturer's instructions. Tartrate-resistant acid phosphatase (TRAP) activity in the culture supernatant was measured by the Osteolinks TRAP assay kit (DS pharma biochemical, Osaka, Japan).

Immunohistochemistry

Paraffin-embedded tissue sections of tuberculosis patients were deparaffinized in xylene, rehydrated in a graded series of ethanol, and immersed in Target Retrieval Solution pH 9.0 (Dako, Glostrup, Denmark) for 20 min boiling for antigen retrieval. Then sections were incubated with 10% normal goat serum to avoid nonspecific reaction, and stained with primary antibodies for 2 h. After inactivating the endogenous peroxidase activity of tissue sections by 3% hydrogen peroxide, the signals were visualized using HRP-conjugated anti-rabbit IgG secondary antibody system (EnVision™+ system, Dako) for 15 min incubation, followed by DAB substrate chromogen system (Dako) with nuclear counterstaining using hematoxylin.

Statistical analysis

The data are presented as the means ± SE and statistical significance was determined with a one-factor factorial ANOVA and Tukey–Kramer's HSD test in the case of multiple comparisons, using the KALEIDAGRAPH® 4.0 program for WINDOWS (Synergy Software, Reading, PA). A significant difference ($P < 0.05$) is indicated with an asterisk and NS indicates nonsignificant differences.

Results and discussion

Living *Mtb* were incorporated and expanded inside multinuclear osteoclasts

It is well known that macrophages are designed to kill pathogens inside the phagosome. After the uptake of pathogens into the macrophages by receptor-mediated phagocytosis, the resulting phagosome undergoes a series of fusion and fission events via the endocytosis pathways. It is believed that osteoclast precursors could be infected with *Mtb* intracellularly, which would be followed by activation in the inflammatory lesions of spinal tissues, as well as activation of a conditional immune response in macrophages. Generally, the pathogenesis of spinal tuberculosis has been reported to rely on an *Mtb*-derived chaperonin protein that induces osteoclast recruitment and inhibits the proliferation of osteoblast precursor cells (Meghji *et al.*, 1997). However, it remains to be elucidated whether *Mtb* has the ability to intracellularly infect multinucleated osteoclasts, although osteoclasts may play an important role in the immunopathogenesis of inflammatory bone diseases.

To investigate whether living *Mtb* were incorporated and expanded inside multinuclear osteoclasts, we cultured living *Mtb* with mature multinuclear osteoclasts (mOCs) and their precursor mononuclear pre-osteoclasts (pMCs) (Fig. 1a). After co-culture with *Mtb*, large numbers of bacteria were incorporated into both mononuclear pMCs and multinuclear mOCs at day 3; in addition, *Mtb*-infected pMCs have ability to multinucleate at day 5 (Fig. 1a). The results indicated that multinuclear osteoclasts also have ability to uptake living *Mtb* inside, as well as mononuclear cells. Next we

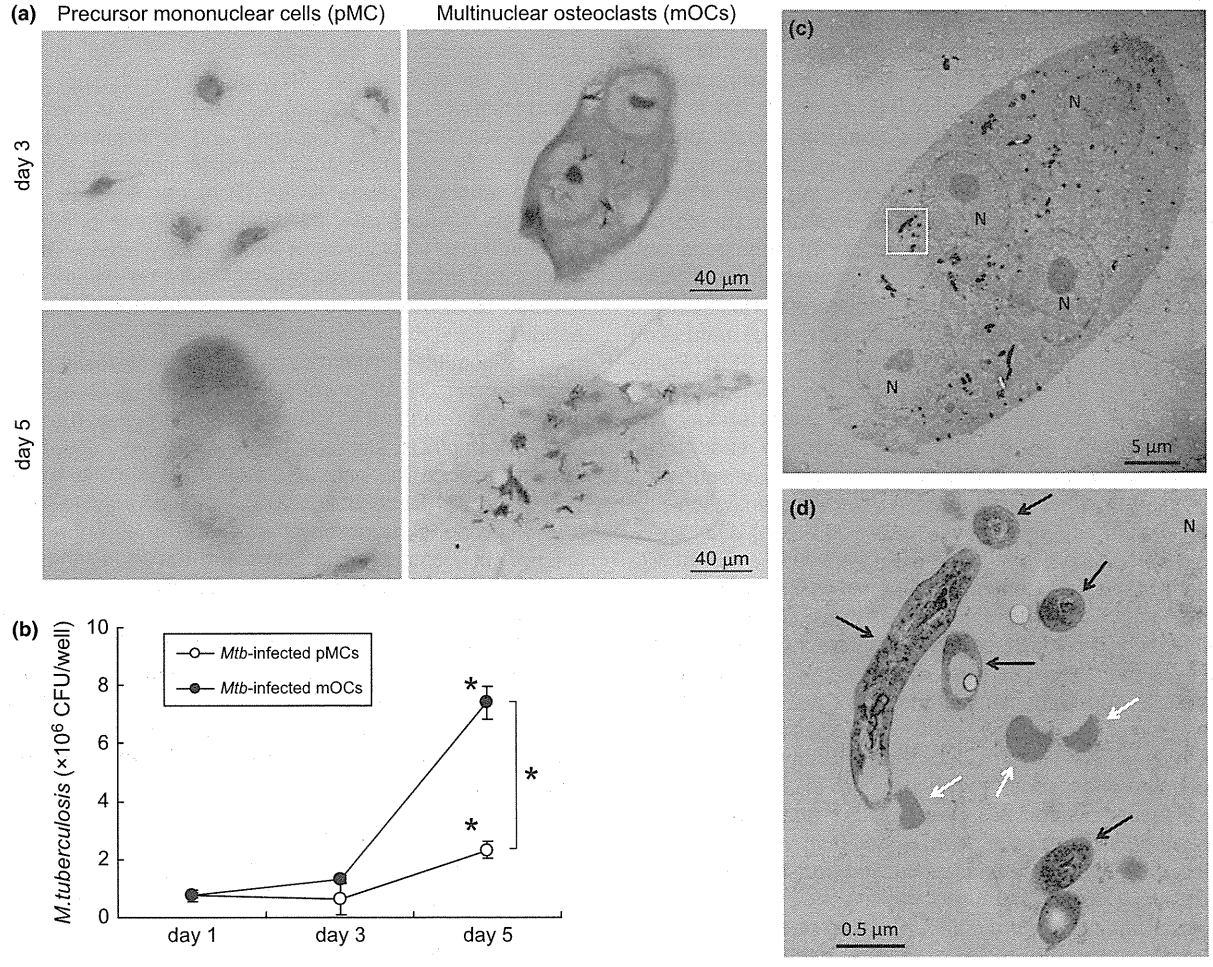

Fig. 1 Intracellular growth of *Mtb* in human mononuclear and multinuclear osteoclasts. (a) Human pMCs and mOCs with living *Mtb* (6.0×10^6 CFU per well) for 3 or 5 days were stained red with Ziehl–Neelsen stain. Nuclei were counterstained with methylene blue. Magnification ×1000 with oil immersion. Scale bar: 40 μm. (b) The CFU numbers of intracellularly infected *Mtb* by pMCs (open column) and mOCs (filled column) were quantified by bacterial culture using a mycobacteria growth indicator glass tube with Ogawa media. (c,d) Electron microscopic images of multinuclear osteoclasts infected with living *Mtb*. The low magnification electron micrograph shows *Mtb* phagocytosed by an mOC (c), and an enlarged image (d) of the area indicated by the rectangle, where five tubercle bacilli reside in the osteoclast cytoplasm without phagosome membrane (black arrrows). Free lysosomes are also distributed in the cytoplasm near tubercle bacilli (white arrows). N, nucleus of the osteoclast.